THE STEADY STATE ANALYSIS OF AC-DC HIGH VOLTAGE POWER TRANSMISSION SYSTEMS

by: I.E. Barker, B.Sc.(Eng.)

A Thesis

Submitted for the Degree of

Master of Philosophy

in the University of Southampton

November 1970.

ABSTRACT

FACULTY OF ENGINEERING AND APPLIED SCIENCE

ELECTRICAL ENGINEERING

Master of Philosophy

THE STEADY STATE ANALYSIS OF AC-DC HIGH VOLTAGE POWER TRANSMISSION SYSTEMS

by Ian Eric Barker

This thesis presents a method of representing the steady state behaviour of a two-terminal H.V.D.C. link for digital computer analysis. The representation is such that it may be used in conjunction with any conventional A.C. load flow program to obtain a simultaneous solution for the operating conditions of both the A.C. system and the associated H.V.D.C. links. The characteristics of the control system of each D.C. link are represented and the operating conditions of each link are defined in terms of the control system settings, i.e. Current Order and Current Margin for a constant current control scheme and Power Order and either Current Margin or Power Margin for constant power control.

The work is developed in three distinct stages. Having established the method of representation and analysis for a single converter station in Chapter 1, Chapter 2 continues to analyse the operation of a complete H.V.D.C. link, assumed to be operating between infinite A.C. system busbars. Chapter 3 proceeds to the complete analysis of an interconnected A.C.-D.C. system.

Computer programs based on the methods described have been written and results obtained using these programs are given for two small test systems.

ACKNOWLEDGEMENTS

The work presented in this thesis was done in the Department of Electrical Engineering of the University of Southampton. I am extremely grateful to Dr. B.A. Carre, my supervisor, for his unfailing advice and encouragement.

I am also indebted to the Nelson Research Laboratories of The English Electric Company for their sponsorship of this work from its inception in October 1964.

CONTENTS

INTRODUCTION

It is becoming increasingly important to be able to represent H.V.D.C. transmission schemes in digital computer programs concerned with all aspects of power system analysis, and at present it would seem that these facilities are most urgently required for load flow, fault level and transient stability programs. This has been brought about simply by the increasing use that is being made of H.V.D.C. power transmission: the very presence of an H.V.D.C. link in a system demands that it should be represented in some way, even if it is of secondary interest in a particular study.

This thesis is concerned only with the steady state or load flow aspects of this problem and presents a method of representing two terminal H.V.D.C. transmission schemes which form part of an integrated A.C.-D.C. power transmission network. Each link is represented in considerable detail: this allows useful studies to be made where the link is of primary importance and the A.C. system is only incidental to the study (e.g. a design study to help determine the tap steps for a converter transformer). Another important feature of the representation is its ability to work in conjunction with any conventional method of load flow analysis.

The method of converter representation used in this thesis is based on the published work of Gavrilovic and Taylor (ref. 1) which gives an account of a method for determining the steady state operating conditions of one terminal of an H.V.D.C. transmission system. The equations are in a per-unit form. This is especially convenient in view of the universal use of per-unit equations for conventional A.C. system representation to which the H.V.D.C. link equations must be coupled.

Chapter 1 examines the methods described by Gavrilovic and Taylor and extends the analysis to deal with an alternative set of constraining terminal conditions which is required for the analysis performed in Chapter 2.

Chapter 2 makes use of the analysis for a single convertor station and proceeds to analyse a two terminal H.V.D.C. link operating between infinite A.C. system busbars. The analysis is complicated by the discontinuities introduced by the characteristics of the control system.

The methods of Chapter 2 are developed in Chapter 3 where an iterative procedure to obtain a simultaneous solution of A.C. and D.C. system variables for an interconnected A.C.-D.C. power transmission network is devised and examined.

Some of the material contained in this thesis has been published previously (ref. 2) by the author, jointly with Dr. R.A. Carre, as an I.E.E. Conference paper in 1966.

CHAPTER 1

ANALYSIS OF A SINGLE H.V.D.C. TERMINAL

1.1 INTRODUCTION.

Converter stations come in many shapes and sizes - so much so that a considerable amount of rationalization is needed before a representation with sufficiently general characteristics can be produced. It would be inconvenient, for example, if different methods of analysis had to be used for two and three winding converter transformers, 6-pulse and 12-pulse bridges, and so on. Rationalization has been achieved to the extent that only a few simple options are required to cover a full range of possible converter station configurations.

The per-unit equations developed by Gavrilovic and Taylor in reference (1) are presented in this chapter but include no reference to an equivalent A.C. system impedance, since for present purposes, only the convertor station itself is of interest. The equations are solved by an iterative method for two sets of constraining terminal conditions - the constraints being those required for the analysis of Chapter 2. The reliability of the iterative procedure is examined and examples of its use are given.

1.2 FEATURES OF THE REPRESENTATION.

1.2.1 Converters.

The basic unit of any H.V.D.C. power transmission scheme is the six-pulse full-wave bridge rectifier: controlled firing angles are essential for inversion but for certain applications diodes may be used for a rectifier terminal. In principle any number of 6-pulse bridges may be connected together in series on the D-C side of the converter and fed in parallel from the A.C. side. Frequently 6-pulse bridges are connected together in this way in one or more pairs, each pair being phase displaced by the converter transformer connections to give 12-pulse operation. A final option for the converter configuration is the possibility of 2 pole operation, achieved by suitable earthing on the D.C. side of the converters.

It is usual for converter stations to be arranged so that each bridge commutates independently of all other bridges - and assuming this to be the case, it has been shown (ref. 1) that for all the above converter arrangements, the basic unit of analysis is a single equivalent 6-pulse bridge. The equivalent bridge is independent of 6 or 12 pulse operation, one or two pole connections or controlled or uncontrolled valves: the number of 6-pulse bridges connected together is of course significant and is involved in the determination of the base values of voltage and power for the per-unit equations on the D.C. side of the converters. Fig. 1 shows a typical bi-polar, 12-pulse converter station having a total of four 6-pulse bridges and indicates the base values to be used for the D.C. side of the converters. A full explanation of the per-unit system for both the A.C. and D.C. sides of the converters is given in reference (1), so it will not be repeated here. Fig. 2 shows the single equivalent 6-pulse bridge and associated per-unit quantities. A list of principal symbols, including those related to Figs. 1 and 2, are given at the end of this thesis.

1.2.2 Converter Transformers.

In the same way as there are many different converter arrangements to be analysed, there are several different converter transformer arrangements. However, for the purposes of the present analysis, factors such as the disposition of the windings on the core, transformer phase shifts etc. do not arise explicitly, the only significant variation being the distinction between a two- and three-winding transformer. The two-winding transformer is treated as a special case of the analysis for a three-winding transformer by a suitable choice of impedances for the star equivalent circuit and by assuming zero injected tertiary current. So again, as for the converters themselves, it is possible to use just one equivalent circuit for all converter transformer arrangements. Fig. 3 shows the full equivalent circuit for the converters and converter transformers and also shows the

filters and static capacitors referred to in the next section.

1.2.3 Reactive Power Supplies and Filters.

Apart from considerations concerning the calculation of commutating reactance, for the purposes of a steady state analysis at the fundamental frequency, filters and static capacitors may both be represented by fixed susceptances. Such susceptances may be connected to either the tertiary winding terminal of a three winding converter transformer or the line winding terminal of a two- or three-winding transformer. Synchronous compensators are usually connected to the tertiary winding of a three-winding transformer and provision has been made to represent them by a fixed reactive power injection at the tertiary terminal of the converter transformer.

1.2.4 Commutating Reactance.

The calculation of commutating reactance depends very much upon the detailed configuration of converter transformers, reactive power supplies and filters. It has been shown (ref. 1) how the commutating reactance may be calculated from the most common converter station configurations, but in order that studies involving unusual configurations may be completed it is felt that the commutating reactance should be given as an independent item of data for any computer program involving steady state converter calculations. An example of an unusual configuration which requires the experienced judgement of an engineer to determine the commutating reactance is the case when no filters are included in the configuration. This may be the case for example at a remote generating station which feeds the main system through a single D-C link, and where the generators have been designed to operate with a high harmonic content.

1.3 FORMULATION OF EQUATIONS.

The equations presented in this section are the basic per-unit equations derived by Gavrilovic and Taylor in reference (1). An additional converter loss term has been added to equation (1) which allows for a voltage drop proportional to the direct current: the

constant arc voltage drop has been neglected.

Equations(1) - (5) define the relationships between the variables for the equivalent circuit of Fig. 2 and equations (6) - (11) refer to Fig. 3.

$$v_d = e_c \operatorname{Cos} \theta - i_d \left(\frac{\pi x_c}{6} + \frac{M\pi^2 r}{18}\right) \tag{1}$$

$$i_p = i_d M \left(v_d + \frac{M\pi^2 i_d r}{18}\right)/e_c \tag{2}$$

$$|\underline{i}_v| \doteq i_d \tag{3}$$

$$i_q = \sqrt{i_d^2 - i_p^2} \tag{4}$$

$$\underline{i}_v = i_p - j\, i_q \tag{5}$$

$$\underline{v}_y = e_c - j\,(x_c - x_v)\underline{i}_v \tag{6}$$

For a susceptance b_t connected to the tertiary winding terminal of the converter transformer,

$$\underline{i}_t = j\underline{v}_y/(x_t - 1/b_t) \tag{7a}$$

For specified reactive power q_t at the tertiary winding terminal of the converter transformer,

$$\underline{i}_t = \left\{ \left[jv_y^2 \left(\sqrt{1 + \frac{4x_t q_t}{v_y^2}} - 1\right)/2x_t \right] \underline{v}_y \right\}^* \tag{7b}$$

or if $x_t = 0$, then

$$\underline{i}_t = (jq_t/\underline{v}_y)^* \tag{7c}$$

and for a two-winding transformer where $x_v = x_t = 0$,

$$\underline{i}_t = 0. \tag{7d}$$

$$\underline{i}_1 = (\underline{i}_v - \underline{i}_t)/n \tag{8}$$

$$\underline{v}_1 = (\underline{v}_y - jnx_1\underline{i}_1)n \tag{9}$$

$$\underline{i}_s = -(\underline{i}_1 + jb_1\underline{v}_1) \tag{10}$$

$$\underline{S} = \underline{v}_1 \underline{i}_s^* \tag{11}$$

1.4 SOLUTION OF EQUATIONS.

If each of the complex variables in equations (1) to (11) are considered as two real variables, then there are fifteen equations in eighteen real variables. This of course means that in order to define a particular operating condition, the equivalent of three real variables must be specified. If the three variables on the right-hand side of equation (1) are specified then all the other variables may be simply evaluated, in turn, in the order defined by equations (1) - (11). This suggests an iterative method of solution of these equations, which in principal could be applied if any three of the eighteen variables are specified. If initial estimates are made for the three variables in the right-hand side of equation (1), say e_{co}, $\cos \theta_o$ and i_{do}, then the following procedure of linear interpolation may be used to obtain the required values for the three specified variables x, y and z of say X, Y, and Z.

(i) Evaluate equations (1) - (11) for the most recently estimated values of e_{co}, $\cos \theta_o$ and i_{do} to obtain the corresponding values of x, y and z, say x_o, y_o and z_o.

(ii) $\delta x := X - x_o$

$\delta y := Y - y_o$

$\delta z := Z - z_o$

(iii) Evaluate equations (1) - (11) for $e_{co} + \Delta e_c$, $\cos \Theta_o$ and i_{do}, where Δe_c is a small displacement in e_{co}, to obtain a numerical approximation to the partial derivatives $\partial x/\partial e_c$, $\partial y/\partial e_c$ and $\partial z/\partial e_c$.

(iv) Evaluate equations (1) - (11) for e_{co}, $\cos \Theta_o + \Delta \cos \Theta$ and i_{do}, where $\Delta \cos \Theta$ is a small displacement in $\cos \Theta$, to obtain a numerical approximation to the partial derivatives $\partial x/\partial \cos \Theta$, $\partial y/\partial \cos \Theta$ and $\partial z/\partial \cos \Theta$.

(v) Evaluate equations (1) - (11) for e_{co}, $\cos \Theta_o$ and $i_{do} + \Delta i_d$, where Δi_d is a small displacement in i_d, to obtain a numerical approximation to the partial derivatives $\partial x/\partial i_d$, $\partial y/\partial i_d$ and $\partial z/\partial i_d$.

(iv) Solve the linear interpolation equations for three variables, equations (12), to determine the necessary displacements to be made to e_{co}, $\cos \Theta_o$ and i_{do} to improve the values of x_o, y_o and z_o i.e. solve equations (12) for δe_c, $\delta \cos \Theta$ and δi_d.

$$\left.\begin{aligned} \delta x &= (\partial x/\partial e_c)\, \delta e_c + (\partial x/\partial \cos \Theta)\, \delta \cos \Theta + (\partial x/\partial i_d)\delta i_d \\ \delta y &= (\partial y/\partial e_c)\, \delta e_c + (\partial y/\partial \cos \Theta)\, \delta \cos \Theta + (\partial y/\partial i_d)\delta i_d \\ \delta z &= (\partial z/\partial e_c)\, \delta e_c + (\partial z/\partial \cos \Theta)\, \delta \cos \Theta + (\partial z/\partial i_d)\delta i_d \end{aligned}\right\} \quad (12)$$

(vii) Having calculated values of δe_c, $\delta \cos \Theta$ and δi_d, then:

$e_{co} := e_{co} + \delta e_c$

$\cos \Theta_o := \cos \Theta_o + \delta \cos \Theta$

$i_{do} := i_{do} + \delta i_d$

Stages (i) - (vii) are repeated in sequence until (ii) gives values of $|\delta x|$, $|\delta y|$ and $|\delta z|$ which are less than a prescribed tolerance, i.e. until the values of X, Y and Z have been attained.

The relationships between e_c, cos Θ, i_d and all the other variables were examined by the author in an attempt to determine the conditions under which the above method would be convergent. However, the general analysis to determine convergence criteria given specified values of any three of the eighteen variables appeared to be very difficult. It also became clear that a study of such a general nature would be of little practical relevance, since work on the operation of a complete two terminal link between infinite A.C. busbars (see Chapter 2) indicated that it would only ever be necessary to specify one of two sets of constraints.

For the two sets of constraints now of vital importance to the complete two-terminal representation, considerable simplification of the generalized procedure proposed in the previous paragraph is possible. For CASE 1, values of i_d and cos Θ are specified and linear interpolation is only required for one variable, e_c, to obtain a specified value of v_1. For CASE 2, i_d is specified and linear interpolation is required for two variables, e_c and cos Θ, to obtain specified values of v_1 and v_d. The necessity for applying these two particular sets of constraints is dealt with in Chapter 2.

For CASE 1, the simplification of the general procedure is extensive and to avoid confusion the resultant procedure is restated here in terms of the specific variables involved rather than in terms of the general variables x, y and z etc.

CASE 1: The values of i_d and cos Θ are specified: assume an initial estimate for e_c, say e_{co}, and then apply the following procedure of linear interpolation to obtain the required value of v_1, say V_1. Initially set $\Delta e_c = -0.1$

(i) Evaluate equations (1) - (9) for e_{co}, i_d and cos Θ, to obtain the corresponding value of v_1, say v_{1o}.

(ii) $\delta v_1 := V_1 - v_{1o}$.

(iii) Evaluate equations (1) - (9) for $e_{co} + \Delta e_c$, i_d and $\cos \Theta$, to obtain a numerical approximation to the partial derivative $\partial v_1 / \partial e_c$.

(iv) Solve the linear interpolation equation for one variable to determine the necessary displacement to be made to e_c to improve the value of v_{1o}. i.e. solve equation (12.1) for δe_c.

$$\delta v_1 = (\partial v_1 / \partial e_c).\delta e_c \qquad (12.1)$$

(v) $e_{co} := e_{co} + \delta e_c$, and

$\Delta e_c := -|\delta e_c|$ if $|\delta e_c| < 0.1$

Stages (i) - (v) are repeated in sequence until (ii) gives a value of $|\delta v_1|$ which is less than a prescribed tolerance, i.e. until the required value of V_1 has been obtained.

For CASE 2, as for CASE 1, considerable simplification of the general procedure is possible and the complete procedure for this case is also given.

CASE 2: The value of i_d is specified: assume initial estimates for e_c and $\cos \Theta$, say, e_{co} and $\cos \Theta_o$ and then apply the following procedure of linear interpolation to obtain the required values of v_1 and v_d, say V_1 and V_d. Initially set $\Delta e_c = -0.1$ and $\Delta \cos \Theta = -0.02$.

(i) Evaluate equations (1) - (9) for e_{co}, $\cos \Theta_o$, and i_d, to obtain the corresponding values of v_1 and v_d, say, v_{1o} and v_{do}.

(ii) $\delta v_1 = V_1 - v_{1o}$

$\delta v_d = V_d - v_{do}$

(iii) Evaluate equations (1) - (9) for $e_{co} + \Delta e_c$, $\cos \Theta_o$, and i_d, to obtain a numerical approximation to the partial derivatives $\partial v_1 / \partial e_c$ and $\partial v_d / \partial e_c$.

(iv) Evaluate equations (1)-(9) for e_{co}, $\cos \Theta_o + \Delta \cos \Theta$, and i_d, to obtain a numerical approximation to the partial derivatives $\partial v_1 / \partial \cos \Theta$ and $\partial v_d / \partial \cos \Theta$.

(v) Solve the linear interpolation equations for two variables to determine the necessary displacement to be made to e_c and $\cos \Theta$ to improve the values of v_1 and v_d, i.e. solve equations (12.2) for δe_c and $\delta \cos \Theta$.

$$\left.\begin{aligned} \delta v_1 &= (\partial v_1 / \partial e_c).\delta e_c + (\partial v_1 / \partial \cos \Theta).\delta \cos \Theta \\ \delta v_d &= (\partial v_d / \partial e_c).\delta e_c + (\partial v_d / \partial \cos \Theta).\delta \cos \Theta \end{aligned}\right\} \quad (12.2)$$

(vi) $e_{co} := e_{co} + \delta e_c$

$\cos \Theta_o := \cos \Theta + \delta \cos \Theta$

$\Delta e_c := -|\delta e_c|$ if $|\delta e_c| < 0.1$

$\Delta \cos \Theta := -|\delta \cos \Theta|$ if $|\delta \cos \Theta| < 0.02$

Stages (i) - (vi) are repeated in sequence until (ii) gives values of $|\delta v_1|$ and $|\delta v_d|$ which are less than a prescribed tolerance.

An investigation into the relationships between the variables involved in the iterative procedures for CASE 1 and CASE 2 has been completed for three typical sets of data referred to as DATA1, DATA2 and DATA3, details of which are given in Table 1. The results show the remarkable linearity of the relationships over the whole range of interest. In fact the relationships between v_d and e_c, $\cos \Theta$ and i_d are in all cases exactly linear, as can be seen from equation (1) and for a two-winding transformer the relationships between v_1 and e_c and between $\cos \Theta$ and i_d are also exactly linear, since for this case

e_c and v_1 are not only linearly related but in certain circumstances are in fact identical quantities. A complete set of graphs relating v_1, v_d, e_c, i_d and cos θ for DATA1, DATA2 and DATA3 are presented in Figs. 4-9 for a full permutation of the following per-unit values of e_c, cos θ, and i_d:

i_d	0.6, 0.8, 1.0
cos θ	0.7, 0.8, 0.9, 1.0
e_c	0.5, 1.0, 1.5

With the exception of Fig. 9 the non-linearities can not easily be seen from these graphs (in fact they exactly linear in some cases). The small degree of non-linearity can however be seen from the tabulations of Tables 2-4.

For the iterative procedure of CASE 2, an important complication is apparent - that is, the value of cos θ can not logically exceed unity. It was at first thought that its calculated value could be allowed to exceed unity for intermediate iterations, and the solution rejected if the final calculated value of cos θ also exceeded unity. This assumption was tried, but it soon became clear that certain limits do in fact apply to cos θ, even for intermediate calculations. It can easily be shown from equations (1) and (2) that if

$$\cos \theta > 1 + \frac{\pi i_d x_c}{6 e_c}$$

then

$$i_p > i_d.$$

Equation (4) will then require the square root of a negative number and fail to produce a meaningful value of i_q. Assuming typical values for i_d, x_c and e_c of 0.8, 0.14 and 1.0 respectively, the limiting value of cos θ is of the order of 1.06. The small margin of 0.06 is insufficient to cater for possible overshoots in the value of cos θ during the intermediate stages of convergence. However an extremely simple solution to this problem has been found as follows:

If, after the solution of equations (12.2), cos θ_o exceeds unity then the new value of cos θ_o is set to unity. If the previous value was also unity then the procedure is terminated and it is assumed that no valid solution exists for the given constraints. By initially setting $\Delta\cos\theta$ negative and ensuring that it remains negative in section (vi) of the procedure for CASE 2, the calculation of partial derivatives in section (iv) can never fail because cos θ is too large. The remote possibility of cos θ_o oscillating against its limit of unity has been guarded against by setting a limit on the number of times equations (12.2) are solved: However this limit (of 10) has never been reached in the very large number of calculations of this type which have now been made. It has not been possible to prove analytically that the process of limiting cos θ_o to unity can not terminate the calculations prematurely, however it has been shown to work reliably in practice. In fact there is an automatic check that the value of cos θ_o has been limited correctly. If a mistake had been made in prematurely assuming that no valid solution exists, then the procedure described in the next chapter would fail to find the appropriate operating condition for the oomplete two terminal link. This has not happened in any case considered to date.

1.5 CONCLUSIONS.

The three sets of test data given in TABLE 1 have been used to obtain the results shown in TABLES 5 and 6. The direct current was 0.8 per-unit in all cases.

TABLE 5 shows the convergence from the initial estimates to typical operating conditions for CASE 1 and CASE 2 when limiting values of cos θ are not involved.

TABLE 6 shows convergence for CASE 2 when the cos θ limit is met.

The example solutions for CASES 1 and 2 are typical of the many other cases studied during the course of the development of several computer programs. Without exception the convergence for both CASE 1

and CASE 2 has been found to be reliable and quick. Because this is so, it is possible to specify fine tolerances for terminating convergence: a value of 10^{-6} p.u. has found to be suitable for all variables and gives a result of comparable precision to an analytical solution of the equations.

The analysis presented in this section is not of great use in its own right, but forms the first logical step in the development of the complete D.C. link representation presented in the next chapter. The analysis for CASES 1 and 2 may in fact be regarded as working subroutines which are available for future analysis.

CHAPTER 2

ANALYSIS OF A TWO TERMINAL H.V.D.C. LINK

2.1 INTRODUCTION.

This chapter establishes how the complete steady state operating condition of a two terminal D.C. link may be determined if control system settings and constant voltages on the A.C. side of the converter transformers are specified.

2.2 FEATURES OF THE REPRESENTATION.

2.2.1 H.V.D.C. Converters.

Each H.V.D.C. terminal is represented as described in Chapter 1.

2.2.2 H.V.D.C. Line.

The D.C. line is represented by a resistance whose value corresponds to the "loop resistance" between the converters.

2.2.3 Control Systems.

Two basic forms of control are considered:

(i) Constant Current Rectifier Control: In this case the inverter angle is held constant and the rectifier firing angle is adjusted to control the magnitude of the current flowing in the D.C. line. If however the rectifier A.C. terminal voltage is too low to permit operation with the rectifier angle above its minimum permissible value, then control passes to the inverter terminal. The inverter firing angle then controls the magnitude of the current in the D.C. line at a lower value, reduced by a specified "current margin", and the rectifier operates at its minimum permissible firing angle.

(ii) Constant Power Rectifier Control: In this case the inverter angle is also held constant and the rectifier firing angle is adjusted to control the power flow at some point along the D.C. line. Again, if the rectifier A.C. terminal voltage is too low to permit operation with the rectifier firing angle above its minimum permissible value, then control passes to the inverter terminal. The inverter firing angle then controls the power

flow in the D.C. line at a lower value, reduced by either a specified "current margin" or "power margin", and the rectifier operates at its minimum permissible firing angle.

Converter transformer tap settings are usually adjusted by the overall control system to maintain rectifier control and nominal D.C. voltage levels. However it has not been possible to consider this particular feature at the present time.

2.3 FORMULATION OF EQUATIONS.

Equations (1) - (11), as derived in section 1.3 are used to represent each terminal. These two sets of equations must then be linked to include the effects of the D.C. line and the overall control system.

The D.C. line is represented by a simple voltage drop equation:

$$v_{dr} - v_{di} = i_d R \qquad (13)$$

The effects of the control system are a little more involved. For constant current control, the direct current i_d is defined by:

$$i_d = i_{do} - \Delta i_d \qquad (14)$$

where i_{do} is the "current order" and Δi_d is the "current margin" which is set to zero when margin conditions do not apply.

For constant power control an additional relationship at one terminal between power order and direct current is required. For constant power control on current margin the required relationship is:

$$i_d = \left[P_{do}/(v_d + Ki_dR)\right] - \Delta i_d \qquad (15a)$$

while for constant power control on power margin the required relationship is:

$$i_d = (P_{do} - \Delta P_d)/(v_d + Ki_dR) \qquad (15b)$$

and in each case $i_{dmax} \geq i_d \geq i_{dmin}$.

P_{do} is the "power order", ΔP_d is the "power margin" and K is a factor which determines the exact point along the D.C. line at which the power is being controlled. The effect of the factor K is to allow for the voltage drop between the converter station to which equation (15a) or (15b) applies and the "control point" on the D.C. line. Table 7 shows the values of K normally used. The appropriate margin

setting, Δi_d or ΔP_d, is set to zero when margin conditions do not apply. The appropriate version of equation (15) is applied to the converter which is not in control in order to determine the value of direct current to be used for equations (1) - (11).

2.4 SOLUTION OF EQUATIONS.

The equations of sections 1.3 and 2.3 are solved together considering first the case for constant current control.

At the inverter terminal the following constraints are known:

$\cos \theta = \cos \gamma_o$

$i_d = i_{do}$

v_1 = specified value.

This corresponds to the CASE 1 solution of equations (1) - (11), as described in section 1.4. Having established the inverter conditions the direct voltage at the rectifier terminal may be obtained by application of equation (13), so at the rectifier the following constraints are known:

$i_d = i_{do}$

v_d = value calculated from equation (13)

v_1 = specified value.

This corresponds to the CASE 2 solution of equations (1) - (11), again as described in section 1.4. The solution is then complete unless no valid solution for CASE 2 can be found, i.e. the A.C. terminal voltage at the rectifier is too low. In this case the link is assumed to be operating under inverter control.

For inverter control under current margin, calculations begin at the rectifier end where the known constraints are:

$\cos \theta = \cos \alpha_o$

$i_d = i_{do} - \Delta i_d$

v_1 = specified value.

Again, CASE 1 of section 1.4 may be used to solve equations (1) - (11), this time for the rectifier terminal, and equation (13) may be used to establish the direct voltage at the inverter terminal. So at the

inverter terminal the known constraints become:

$i_d = i_{do} - \Delta i_d$

v_d = value calculated from equation (13)

v_1 = specified value.

Then CASE 2 of section 1.4 may be applied again to determine the conditions at inverter, and will in the vast majority of cases yield a satisfactory solution. However, it is theoretically possible when working under current margin conditions for the A.C. terminal voltage to be too low to allow the rectifier angle to exceed α_o. The true operating condition in such cases corresponds to a direct current in the range

$$i_{do} > i_d > i_{do} - \Delta i_d.$$

The value of i_d may be determined by simple linear interpolation for i_d, using constant converter control angles of γ_c and α_o at the inverter and rectifier, and beginning with a value of i_d half way between i_{do} and $i_{do} - \Delta i_d$. This procedure can only fail to determine a value of i_d if the method of dealing with Cos θ limits for CASE 2 as described in section 1.4 has also failed.

The overall procedure for constant power control is identical to that just described for constant current control with the single exception that for the converter that is not in control the appropriate version of equation (15) is solved simultaneously with equation (1), to determine the value of direct current.

Solution with equation (15a) yields:

$$i_d = \frac{(\Delta i_d.B-A-\Delta i_d KR)+\sqrt{(A-\Delta i_d B+\Delta i_d KR)^2+4(B-KR)(A.\Delta i_d-P_{do})}}{2(KR-B)} \qquad (16a)$$

$$i_{dmax} \geq i_d \geq i_{dmin}.$$

Solution with equation (15b) yields:

$$i_d = \frac{-A + \sqrt{A^2 + 4\,(B-KR)\,(\Delta P_d - P_{do})}}{2\,(KR-B)} \qquad (16b)$$

$$i_{dmax} \geq i_d \geq i_{dmin}.$$

In each case,

$$A = e_c \cos \theta$$

$$B = \frac{\pi x_c}{6} + \frac{M\pi^2 r}{18}$$

and Δi_d or ΔP_d is set to zero if margin conditions do not apply.

2.5 CONCLUSIONS.

The procedures described in this chapter were used to produce a program to study the inter-relation between the various data constants and control system settings. The program was not however used in this way but in fact became a subroutine used in the analysis described in Chapter 3. A version of the routine in the form of a separate program, rather than a subroutine, was however retained, and would have become a vital tool had it become necessary to investigate failures in the convergence of the overall A.C./D.C. system analysis described in the next chapter.

No example solutions that specifically illustrate the methods described in this chapter have been obtained, but their validity is demonstrated indirectly by the results given in the next chapter for overall A.C./D.C. system studied.

CHAPTER 3

ANALYSIS OF A PARALLEL A.C.-D.C. TRANSMISSION SYSTEM

3.1 INTRODUCTION.

Assuming given control system settings and A.C. terminal voltages at each end of a D.C. link, Chapter 2 describes how the operating conditions of a link, including the real and reactive power transfer at each terminal, may be established. This immediately suggests an iterative method of solution of the following type for the simultaneous set of equations describing an interconnected A.C.-D.C. transmission system:

(i) Initially, the A.C. system busbar voltages are estimated, and then the two following calculations are performed alternately until all changes in A.C. system busbar voltages are smaller than a prescribed tolerance.

(ii) Using the latest estimates of the A.C. busbar voltages at the terminals of each D.C. link in the network together with the various control system settings, calculate the real and reactive power transfers to the A.C. network by the method described in Chapter 2.

(iii) Using these power transfers, improve the estimates of all A.C. busbar voltages using any conventional A.C. load flow method.

This approach has also been used for the network analyser and is described in reference (3). It has also been found successful for digital calculation and details of a program based on this method are described in this chapter. The program was originally written by the author in PEGASUS AUTOCODE for the Southampton University PEGASUS computer and then subsequently re-written in KDF9 USERCODE. The USERCODE version of the program completed in March, 1966, is now in regular use by the Power Systems Department, English Electric Power Transmission Limited, Stafford.

3.2 FEATURES OF THE REPRESENTATION.

3.2.1 The A.C. System.

The representation of the A.C. system allows the passive network to be built up from series lines in the form of nominal π circuits, two winding transformers with off nominal taps, and shunt impedances. Multi-winding transformers can be represented by the appropriate equivalent circuit consisting of two or more two winding transformers and series lines. Terminal constraints at generation points are specified in terms of fixed voltage modulus and angle at any number of slack busbars, fixed real power injection and voltage modulus at voltage regulated nodes, and by fixed real and reactive power injection. Loads of fixed real and reactive power may be specified at any busbar.

Apart from the provision of more than one slack busbar, this specification corresponds to that normally made for A.C. load flow programs. Having more than one slack allows the program to be used for short time regulation studies (i.e. up to about 0.2 seconds after a disturbance) on the basis that:

(i) Automatic voltage regulating equipment has not had time to act and so each machine may be represented by a fixed complex voltage (i.e. a slack busbar) behind the machines direct-axis transient reactance.

(ii) Load may be represented as fixed impedances to ground and A.C. system faults as low impedance shunts.

(iii) Automatic transformer tap changers have not operated.

(iv) D.C. link control systems operate instantly.

(v) If either equation (7b) or (7c) has been applied to the steady state operation of the link, then it is replaced by:

$$i_t = (\underline{e}_b - \underline{v}_t)/j\,(x_t + x_b') \qquad (7e)$$

where $\underline{e}_b$ is the emf behind the direct axis transient reactance of the synchronous compensator, x'_b.

3.2.2 The D.C. Links.

The D.C. links are represented as described in Chapter 2.

3.3 FORMULATION OF EQUATIONS.

The equations for the A.C. System may be derived by considering the generalized non-slack node, i, in the network where there may be connections to adjacent nodes, j, slack nodes, s, and to earth, o. Applying Kirchoff's current law for a net complex power injection $\underline{S}_i$, which may be from a combination of various load and/or generation representations,

$$\underline{V}_i \left[\sum_j \underline{Y}_{ij} + \sum_o \underline{Y}_{io} + \sum_s \underline{Y}_{is} \right] - \sum_j \underline{Y}_{ij}\underline{V}_j - \sum_s \underline{Y}_{is}\underline{V}_s = \left(\frac{\underline{S}_i}{\underline{V}_i} \right)^* \qquad (17)$$

or

$$\underline{V}_i = \left[\left(\frac{\underline{S}_i}{\underline{V}_i} \right)^* + \sum_s \underline{Y}_{is}\underline{V}_s + \sum_j \underline{Y}_{ij}\underline{V}_j \right] / \underline{Y}_{ii} \qquad (18)$$

Transformers are included, effectively in the equivalent π circuit form, and so contribute to both the $\underline{Y}_{ij}$ and $\underline{Y}_{io}$ terms of equations (17).

The equations for voltage regulated busbars cannot be explicitly formulated at this stage since they depend upon the method of solution chosen for the A.C. system. In all cases however, the principal is to adjust the value of injected reactive power, possibly between fixed limits, in order to achieve the specified voltage modulus.

The equations for the D.C. links are formulated as described in Chapter 2.

3.4 SOLUTION OF EQUATIONS.

Of the three stages of the overall method of solution outlined in section 3.1, stage (i) needs no further explanation, and stage (ii)

has been dealt with fully in Chapter 2. It only remains therefore to discuss the solution of the A.C. network equations and the convergence of the overall scheme.

In principal, any Load Flow method which allows for the specification of net real and reactive power at any busbar may be used with the D.C. link representation described. The choice of method is therefore quite open. In general however, it would seem that the nodal iterative methods offer more flexibility in that the "degree of improvement" of A.C. network voltages for the latest power transfers to and from a D.C. link is under fine control and this could lead to a more efficient solution. For this reason a Successive Over-Relaxation (S.O.R.) nodal iterative method was chosen in which the same real accelerating factor, ω , is used for both real and imaginary components of complex voltage.

The S.O.R. procedure for the $(m+1)^{th}$ iteration may be defined as:

$$\underline{V}_i^{(m+1)} = \underline{V}_i^{(m)} + \omega\left[\left(\frac{\underline{S}_i^{(m)}}{\underline{Y}_{ii}^{*}} \Big/ \underline{V}_i^{(m)}\right)^{*} + \sum_{s} \frac{\underline{Y}_{is}\underline{V}_s}{\underline{Y}_{ii}} + \sum_{j<i} \frac{\underline{Y}_{ij}\underline{V}_j^{(m+1)}}{\underline{Y}_{ii}} + \sum_{j>i} \frac{\underline{Y}_{ij}\underline{V}_j^{(m)}}{\underline{Y}_{ii}} - \underline{V}_i^{(m)}\right] \quad (19)$$

Busbar voltage regulation is achieved by variation of the net reactive power injected at a machine busbar while the real power is held constant. Thus for a voltage regulated busbar i, P_i and V_i are specified. After the application of equation (19) for busbar i at each iteration, the reactive component, Q_i, of $\underline{S}_i^{(m)}$ is adjusted on the basis that adjacent busbar voltages are not changed by the modified reactive power injection. A corresponding adjustment is then also made to $\underline{V}_i^{(m+1)}$.

After the application of equation (19), the net current injection at node i, $\underline{I}_i^{(m+1)}$ corresponding to $\underline{S}_i^{(m)}$, becomes $\left[\underline{S}_i^{(m)}/\underline{V}_i^{(m+1)}\right]^{*}$,

$$\text{So,} \quad \underline{S}_i^{(m)} = \underline{v}_i^{(m+1)} \left[\underline{i}_i^{(m+1)} \right]^* \tag{20}$$

If the change in Q_i, ΔQ_i, is assumed not to modify the values of $\underline{v}_j$ at adjacent nodes, but causes a voltage change of $\Delta \underline{v}_i^{(m+1)}$ at node i,

$$\text{then} \quad \underline{S}_i^{(m+1)} = \left[v_i^{(m+1)} + \Delta \underline{v}_i^{(m+1)} \right] \cdot \left[\underline{i}_i^{(m+1)} + \Delta \underline{v}_i^{(m+1)} \underline{Y}_{ii} \right]^*, \tag{21}$$

$$\text{and} \quad \Delta \underline{S}_i^{(m+1)} = \underline{S}_i^{(m+1)} - \underline{S}_i^{(m)} \tag{22}$$

$$= \Delta P_i^{(m+1)} + j \Delta Q_i^{(m+1)}. \tag{23}$$

So, from equations (20) - (22), and neglecting terms in $\Delta \underline{v}_i^2$,

$$\Delta S_i^{(m+1)} = \underline{v}_i^{(m+1)} \left[\Delta \underline{v}_i^{(m+1)} \underline{Y}_{ii} \right]^* + \Delta \underline{v}_i^{(m+1)} \left[\underline{i}_i^{(m+1)} \right]^* \tag{24}$$

$$\text{Given} \quad V_i = \left| \left\{ \underline{v}_i^{(m+1)} + \Delta \underline{v}_i^{(m+1)} \right\} \right| \tag{25}$$

$$\text{and} \quad \Delta P_i^{(m+1)} = 0 \tag{26}$$

the required values of $\Delta Q_i^{(m+1)}$ and $\Delta \underline{v}_i^{(m+1)}$ may be determined from equations (23)-(26).

If $\underline{v}_i^{(m+1)} = e + jf$

$\underline{i}_i^{(m+1)} = a + jb$

$\underline{Y}_{ii} = G + jB$

$\Delta \underline{v}_i^{(m+1)} = x + jy,$

then, again neglecting terms in $\Delta \underline{v}_i^2$,

$$x = (V_i^2 - e^2 - f^2)/2 \ (e + fk) \tag{27}$$

$$y = kx \tag{28}$$

where $k = (eG + fB + a)/(eB - fG - b),$

and $$\Delta Q_i^{(m+1)} = x\,(fG - eB - b) + y\,(a - fB - eG). \qquad (29)$$

If $Q_i max < Q_i^{(m+1)}$ or if $Q_i^{(m+1)} < Q_i min$, the limiting value of Q_i, Q_{limit}, is used and the displacement $\Delta \underline{v}_i^{(m+1)}$ to be applied to the latest voltage estimate, $\underline{v}_i^{(m+1)}$, is proportionately reduced, thus:

$$\Delta \underline{v}_i^{(m+1)} := \Delta \underline{v}_i^{(m+1)} \cdot \left[\left| \frac{(Q_i^{(m)} - Q_{limit}}{\Delta Q_i^{(m+1)}} \right| \right] \qquad (30)$$

An important point to consider in the convergence of the overall procedure is the effect of the discontinuity introduced when D.C. links are switched over to operation under inverter control under margin conditions after the initial assumption that they are operating under rectifier control. The apparent need for inverter control may only be due to incomplete convergence of the A.C. system voltages, and the premature selection of margin operation for any D.C. link would have a detrimental effect on the overall convergence. Indeed, with more than one D.C. link behaving in this way, convergence may be prevented altogether. For this reason it was decided to divide the calculation into two phases:

Phase 1. Maintain Δi_d or ΔP_d equal to zero for all D.C. links during inverter control calculations until a converged solution for the overall A.C.-D.C. system has been achieved.

Phase 2. If any D.C. link is on inverter control then continue the calculations allowing true values of Δi_d or ΔP_d to be used for all D.C. links during inverter control calculations.

3.5 CONCLUSIONS.

Two test systems were used to study the performance of the method.

The first trials were made using a simple 4 busbar network, details of which are given in Table 8 and Fig. 10. Three studies

were performed to determine what effect the relative strength of the parallel A.C. and D.C. ties had on the overall convergence process. The direct current order was changed for each study: values of i_{do} = 0.3, 0.5 and 0.7 per-unit were used, giving ratios of A.C. to D.C. power transfer of 2.57, 1.22 and 0.61 respectively. Rectifier control was maintained in each case. In order to eliminate the effects of the particular method chosen for the solution of the A.C. network equations, the S.O.R. iterations were allowed to continue until a well converged solution was obtained between each D.C. link calculation. Convergence was equally rapid in each case. Fig. 12 shows how the rectifier and inverter A.C. terminal voltages converge to within 0.0005 p.u. of the asymptotic value after five D.C. link calculations in each case.

Having demonstrated considerable insensitivity to the relative strengths of parallel A.C. and D.C. ties, which is essential to the satisfactory operation of the method in the general case, further investigations were made using a second test system shown in Fig. 11.

The 14 busbar systems of Fig. 11 is an I.E.E.E. Computer Applications Sub-Committee Standard system in which a strong A.C. connection which carried 61.7 MW has been replaced by a D.C. link designed to transmit the same power and maintain the voltages throughout the A.C. system. The data for the A.C. system is given in Table 9 and the data used for the D.C. link is given in Table 10. The convergence from an initial estimate of 1 p.u. at all busbars for this A.C.-D.C. system was examined in seven test runs, in which the number of S.O.R. iterations between D.C. link calculations was varied for each run. In the last run no D.C. link calculations are performed after the initial calculation: this therefore corresponds to a normal A.C. load flow in which the D.C. link is replaced by constant real and reactive power generation - the complex power at each terminal corresponding to that injected by the D.C. link for terminal voltages

of 1 p.u. Figures 13-19 show how the voltage voltage displacements at the rectifier and inverter terminals vary between successive S.O.R. iterations for each of the seven test runs.

Two important conclusions may be drawn from these Figures. Firstly that the relative frequency of S.O.R. iterations and D.C. link calculations is not critical, and secondly that convergence rates and numbers of S.O.R. iterations required for A.C.-D.C. and conventional A.C. load flow studies (Fig. 19) are almost the same. Table 11 gives a summary of data relevant to these conclusions.

A careful study of the Electrical section of Science Abstracts shows that since the completion of the original work for this thesis in October 1965, very little published work has appeared which directly relates to the work described here. References (4) and (5), published at about the same time as the authors own paper, reference (2), both use methods very similar to those described here.

References 6 and 7 perhaps indicate the direction in which interest in the subject is moving and are typical of several papers on multi-terminal D.C. links, in that more attention is given to the logic of the control systems proposed than to the performance of the mathematical methods devised. In particular, it may prove quite difficult under certain circumstances to decide which mode each link is operating in, if, during the convergence of the overall process, the relative values of A.C. terminal voltages for each link are substantially in error.

REFERENCES

1. Gavrilovic, A. and Taylor, D.G. 'The calculation of Regulation Characteristics of D.C. Transmission Systems'. I.E.E.E. Trans. on Power App. and Systems, 1964, 83, p.215.

2. Barker, I.E. and Carre, B.A. 'Load Flow Calculations for Systems Containing H.V.D.C. Links'. I.E.E. Conference Publication: High Voltage D.C. Transmission 19th - 23rd September, 1966, Part I, p.115.

3. Uhlmann, E. 'The Representation of an H.V.D.C. Link in a Network Analyser'. C.I.G.R.E. Paper No. 404, 1960.

4. Hingorani, N.G. and Mountford, J.D. 'Simulation of H.V.D.C. Systems in A.C. Load-flow Analysis by Digital Computer'. Proc. I.E.E. (G.B.) Vol. 113, No. 9, 1541-6 (Sept. 1966).

5. Breuer, G.D., Luini, J.F. and Young, C.C. 'Studies of large A.C.-D.C. Systems on the Digital Computer'. I.E.E.E. Trans Power Apparatus Syst. (U.S.A.) Vol. PAS 85, No. 11, 1107-16 (Nov. 1966).

6. Norton, J.P. and Corey, B.J. 'Digital Simulation Program for Multi-terminal H.V.D.C. Systems'. Proc. Instn. Elect. Eng. (G.B.) Vol. 115, No. 3, 397-406 (March 1968).

7. Dougherty, J.J. 'Operating characteristics of a Three Terminal D.C. Transmission Line'. I.E.E.E. Trans. Power Apparatus Syst. (U.S.A.) Vol. PAS 89, No. 5-6, 775-80 (March 1968).

PRINCIPAL SYMBOLS

Complex quantities are underlined, thus $\underline{v}$

Complex conjugate is indicated, thus $\underline{v}^*$

Modulus value of complex numbers and real numbers are indicated, thus v.

D.C. System.

v_d	Converter Direct Voltage, p.u.
e_c	Commutating Voltage, p.u.
α	Rectifier firing angle, degrees.
γ	Inverter margin Angle, degrees.
θ	General firing Angle/margin Angle, degrees.
i_d	Direct current, p.u.
x_c	Commutating reactance, p.u.
r	Converter "loss resistance", p.u.
M	Marker, +1 Rectifier, -1 Inverter.
$\underline{i}_v$	Valve winding current, p.u.
i_p	In phase component of $\underline{i}_v$, p.u.
i_q	Quadrature component of $\underline{i}_v$, p.u.
x_v	Converter transformer valve winding reactance, p.u.
x_t	Converter transformer tertiary winding reactance, p.u.
x_l	Converter transformer line winding reactance, p.u.
$\underline{i}_t$	Converter transformer tertiary winding current, p.u.
$\underline{v}_y$	Converter transformer starpoint voltage, p.u.
$\underline{v}_l$	D.C. link A.C. terminal voltage, p.u.
$\underline{i}_l$	Converter transformer line winding current, p.u.
$\underline{i}_s$	D.C. Link current injection into A.C. network, p.u.
$\underline{S}$	Complex power injection into A.C. network, p.u.
i_{do}	Current order for constant current control, p.u.
Δi_d	Current margin, p.u.
P_{do}	Power order for constant power control p.u.
ΔP_d	Power margin, p.u.
R	D.C. line (loop) resistance, p.u.

n Converter transformer line winding tap setting, p.u.

α_o Min value α, degrees.

γ_o Min value γ, degrees.

q_t Reactive power injection at converter transformer tertiary, p.u.

$\underline{e}_b$ Internal emf of synchronous machine on tertiary winding of converter transformer, p.u.

x'_b Direct axis transient reactance of synchronous machine on tertiary winding of converter transformer, p.u.

$\underline{v}_t$ Converter transformer tertiary winding terminal voltage, p.u.

b_t Susceptance of shunt capacitor connected to converter transformer tertiary winding terminal, p.u.

b_l Susceptance of shunt capacitor connected to D.C. link terminal point, p.u.

N Number of bridges connected in series on D.C. side of converter.

V_v Converter transformer valve winding nominal voltage, volts.

MVA_t Converter transformer rating, MVA.

See also Fig. 3 for D.C. link notation.

A.C. System.

$\underline{Y}$ Admittance, p.u.

$\underline{v}$ Busbar voltage, p.u.

V Specified busbar voltage modulus, p.u.

P Real power, p.u. (net injection to A.C. network).

Q Reactive power, p.u. (net injection to A.C. network).

$\underline{S}$ Complex power, $P + jQ$, p.u. (net injection to A.C. Network).

$\underline{i}$ Current corresponding to complex power $\underline{S}$, p.u.

TABLE 1

Basic Converter Data used for Numerical Examples

DATA 1	Two-winding transformer	$x_c = 0.18$
		$x_v = 0.18$
		$x_t = 0$
		$x_l = 0$
		$n = 1.0$
		$b_t = 0$
		$q_t = 0$
DATA 2	Three-winding transformer,	$x_c = 0.085$
	with tertiary filter.	$x_v = 0.08$
		$x_t = 0.005$
		$x_l = 0.08$
		$n = 1.0$
		$b_t = 0.35$
		$q_t = 0$
DATA 3	Three-winding transformer,	$x_c = 0.15$
	with tertiary synchronous	$x_v = 0.08$
	compensator.	$x_t = 0.005$
		$x_l = 0.08$
		$n = 1.0$
		$b_t = 0$
		$q_t = 0.35$

All data in per-unit on 100 MVA base.

TABLE 2

Tabulation of relationships of Figs. 4 and 5 for DATA 1.

e_c	cos θ	i_d	v_d	v_i
0.500000	0.700000	0.600000	0.293451	0.500000
1.000000	0.700000	0.600000	0.643451	1.000000
1.500000	0.700000	0.600000	0.993451	1.500000
0.500000	0.700000	0.800000	0.274602	0.500000
1.000000	0.700000	0.800000	0.624602	1.000000
1.500000	0.700000	0.800000	0.974602	1.500000
0.500000	0.700000	1.000000	0.255752	0.500000
1.000000	0.700000	1.000000	0.605752	1.000000
1.500000	0.700000	1.000000	0.955752	1.500000
0.500000	0.800000	0.600000	0.343451	0.500000
1.000000	0.800000	0.600000	0.743451	1.000000
1.500000	0.800000	0.600000	1.143451	1.500000
0.500000	0.800000	0.800000	0.324602	0.500000
1.000000	0.800000	0.800000	0.724602	1.000000
1.500000	0.800000	0.800000	1.124602	1.500000
0.500000	0.800000	1.000000	0.305752	0.500000
1.000000	0.800000	1.000000	0.705752	1.000000
1.500000	0.800000	1.000000	1.105752	1.500000
0.500000	0.900000	0.600000	0.393451	0.500000
1.000000	0.900000	0.600000	0.843451	1.000000
1.500000	0.900000	0.600000	1.293451	1.500000
0.500000	0.900000	0.800000	0.374602	0.500000
1.000000	0.900000	0.800000	0.824602	1.000000
1.500000	0.900000	0.800000	1.274602	1.500000
0.500000	0.900000	1.000000	0.355752	0.500000
1.000000	0.900000	1.000000	0.805752	1.000000
1.500000	0.900000	1.000000	1.255752	1.500000
0.500000	1.000000	0.600000	0.443451	0.500000
1.000000	1.000000	0.600000	0.943451	1.000000
1.500000	1.000000	0.600000	1.443451	1.500000
0.500000	1.000000	0.800000	0.424602	0.500000
1.000000	1.000000	0.800000	0.924602	1.000000
1.500000	1.000000	0.800000	1.424602	1.500000
0.500000	1.000000	1.000000	0.405752	0.500000
1.000000	1.000000	1.000000	0.905752	1.000000
1.500000	1.000000	1.000000	1.405752	1.500000

All values in per-unit.

TABLE 3

Tabulation of relationships of Figs. 6 and 7 for DATA 2

e_c	Cos Θ	i_d	v_d	v_i
0.500000	0.700000	0.600000	0.323296	0.521183
1.000000	0.700000	0.600000	0.673296	1.005743
1.500000	0.700000	0.600000	1.023296	1.491208
0.500000	0.700000	0.800000	0.314395	0.534056
1.000000	0.700000	0.800000	0.664395	1.017662
1.500000	0.700000	0.800000	1.014395	1.502759
0.500000	0.700000	1.000000	0.305494	0.547388
1.000000	0.700000	1.000000	0.655494	1.029875
1.500000	0.700000	1.000000	1.005494	1.514523
0.500000	0.800000	0.600000	0.373296	0.517066
1.000000	0.800000	0.600000	0.773296	1.001143
1.500000	0.800000	0.600000	1.173296	1.486434
0.500000	0.800000	0.800000	0.364395	0.528954
1.000000	0.800000	0.800000	0.764395	1.011752
1.500000	0.800000	0.800000	1.164395	1.496549
0.500000	0.800000	1.000000	0.355494	0.541456
1.000000	0.800000	1.000000	0.755494	1.022756
1.500000	0.800000	1.000000	1.155494	1.506951
0.500000	0.900000	0.600000	0.423296	0.511397
1.000000	0.900000	0.600000	0.873296	0.994695
1.500000	0.900000	0.600000	1.323296	1.479690
0.500000	0.900000	0.800000	0.414395	0.521995
1.000000	0.900000	0.800000	0.864395	1.003522
1.500000	0.900000	0.800000	1.314395	1.487823
0.500000	0.900000	1.000000	0.405494	0.533429
1.000000	0.900000	1.000000	0.855494	1.012901
1.500000	0.900000	1.000000	1.305494	1.496360
0.500000	1.000000	0.600000	0.473296	0.502328
1.000000	1.000000	0.600000	0.973296	0.983280
1.500000	1.000000	0.600000	1.473296	1.467064
0.500000	1.000000	0.800000	0.464395	0.511311
1.000000	1.000000	0.800000	0.964395	0.989548
1.500000	1.000000	0.800000	1.464395	1.472116
0.500000	1.000000	1.000000	0.455494	0.521478
1.000000	1.000000	1.000000	0.955494	0.996707
1.500000	1.000000	1.000000	1.455494	1.477894

All values in per-unit.

TABLE 4

Tabulation of relationships of Figs. 8 and 9 for DATA 3.

e_c	Cos Θ	i_d	v_d	v_l
0.500000	0.700000	0.600000	0.302876	0.445466
1.000000	0.700000	0.600000	0.652876	0.975713
1.500000	0.700000	0.600000	1.002876	1.485427
0.500000	0.700000	0.800000	0.287168	0.445802
1.000000	0.700000	0.800000	0.637168	0.977019
1.500000	0.700000	0.800000	0.987168	1.486856
0.500000	0.700000	1.000000	0.271460	0.446087
1.000000	0.700000	1.000000	0.621460	0.978359
1.500000	0.700000	1.000000	0.971460	1.488317
0.500000	0.800000	0.600000	0.352876	0.445474
1.000000	0.800000	0.600000	0.752876	0.975252
1.500000	0.800000	0.600000	1.152876	1.484864
0.500000	0.800000	0.800000	0.337168	0.445883
1.000000	0.800000	0.800000	0.737168	0.976439
1.500000	0.800000	0.800000	1.137168	1.486131
0.500000	0.800000	1.000000	0.321460	0.446274
1.000000	0.800000	1.000000	0.721460	0.977677
1.500000	0.800000	1.000000	1.121460	1.487441
0.500000	0.900000	0.600000	0.402876	0.445455
1.000000	0.900000	0.600000	0.852876	0.974615
1.500000	0.900000	0.600000	1.302876	1.484081
0.500000	0.900000	0.800000	0.387168	0.445938
1.000000	0.900000	0.800000	0.837168	0.975645
1.500000	0.900000	0.800000	1.287168	1.485131
0.500000	0.900000	1.000000	0.371460	0.446442
1.000000	0.900000	1.000000	0.821460	0.976748
1.500000	0.900000	1.000000	1.271460	1.486241
0.500000	1.000000	0.600000	0.452876	0.445371
1.000000	1.000000	0.600000	0.952876	0.973580
1.500000	1.000000	0.600000	1.452876	1.482737
0.500000	1.000000	0.800000	0.437168	0.445929
1.000000	1.000000	0.800000	0.937168	0.974408
1.500000	1.000000	0.800000	1.437168	1.483486
0.500000	1.000000	1.000000	0.421460	0.446547
1.000000	1.000000	1.000000	0.921460	0.975344
1.500000	1.000000	1.000000	1.421460	1.484333

All values in per-unit.

TABLE 5

Convergence for CASE 1 and CASE 2 not involving Cos θ limits

DATA	CASE	e_c	cos θ	v_d	v_l
1	1	0.900000	-	-	0.900000
		0.950000	0.965926	0.842231	(0.950000)
1	2	0.900000	0.990000	0.815602	0.900000
		0.950000	0.964588	0.840961	0.950000
		0.950000	0.965926	(0.842231)	(0.950000)
2	1	0.900000	-	-	0.899166
		0.952790	-	-	0.950066
		0.952722	0.965926	0.884695	(0.950000)
2	2	0.900000	0.990000	0.855395	0.895270
		0.952816	0.964411	0.883302	0.950265
		0.952781	0.965866	0.884654	0.950019
		0.952722	0.965926	(0.884695)	(0.950000)
3	1	0.900000	-	-	0.871779
		0.975249	-	-	0.949449
		0.975781	-	-	0.949996
		0.975785	0.965926	0.879704	(0.950000)
3	2	0.900000	0.990000	0.828168	0.871474
		0.975309	0.964422	0.877777	0.949529
		0.975783	0.965928	0.879704	0.949999
		0.975785	0.965926	(0.879704)	(0.950000)

The constraining values of v_d and v_l to be achieved are given in brackets. Convergence in all cases is complete to six figures. All values in per-unit.

TABLE 6

Convergence for CASE 2 involving Cos Θ limits

DATA	CASE	e_c	cos Θ	v_d	v_l
1	2	0.900000	0.990000	0.815602	0.900000
		0.950000	1.000000	0.874602	0.950000
		0.950000	1.000000	0.874602	0.950000
				(0.909846)	(0.950000)
2	2	0.900000	0.990000	0.855395	0.895270
		0.963483	1.000000	0.927878	0.954406
		0.969050	1.000000	0.933445	0.959762
				(0.954719)	(0.950000)
3	2	0.900000	0.990000	0.828168	0.871474
		0.976067	1.000000	0.913235	0.949798
		0.976965	1.000000	0.914133	0.950722
				(0.945504)	(0.950000)

The constraining values of v_d and v_l which were to have been achieved are given in brackets. All values in per-unit.

TABLE 7

Values of K for Constant Power Control

Equations (15a) and (15b)

Station in Control	Control Point on D.C. line	K
RECTIFIER	RECTIFIER END	1
RECTIFIER	INVERTER END	0
RECTIFIER	CENTRE	0.5
INVERTER	RECTIFIER END	0
INVERTER	INVERTER END	-1
INVERTER	CENTRE	-0.5

TABLE 8

D.C. Link Data for 4 Busbar Test System

	Inverter	Rectifier
b_l	0.0950	0.0950
x_l	0.0705	0.0700
x_v	0.0800	0.0700
x_t	0.0010	0.0010
b_t	0.1000	0.1000
y_o	10	-
α_o	-	0
n	1.0300	0.9900
$\bar{x}_c$	0.1510	0.1405

D.C. line resistance, R = 0.03

Current margin setting, Δi_d = 0

All values in per-unit on 100 MVA base.

TABLE 9

A.C. System Data for 14 Busbar Test System.

Branch Data

end 1	end 2	Total Series Impedance		Total line susceptance	Transformer Tap ratio n (end1/end2)
		R	X	B	
2	3	0.04699	0.19797	0.0438	-
2	4	0.05811	0.17632	0.0374	-
2	5	0.05695	0.17388	0.0340	-
3	4	0.06701	0.17103	0.0346	-
4	7	0	0.20912	0	0.978
4	9	0	0.55618	0	0.969
5	6	0	0.25202	0	0.932
6	11	0.09498	0.19890	0	-
6	12	0.12291	0.25581	0	-
6	13	0.06615	0.13027	0	-
7	8	0	0.17615	0	-
7	9	0	0.11001	0	-
9	10	0.03181	0.08450	0	-
9	14	0.12711	0.27038	0	-
10	11	0.08205	0.19207	0	-
12	13	0.22092	0.19988	0	-
13	14	0.17093	0.34802	0	-
9	0	0	-5.26316	0	-
2	1	0.01938	0.05917	0.0528	-
5	1	0.05403	0.22304	0	-

Nodal Data

Busbar	Type	LOAD				GENERATION		
		MW	MVAr	V%	θ^{o}	MW	MVAr max	MVAr min
1	Slack	0	0	106.0	0	-	-	-
2	PV	21.7	12.7	104.5	-	40.0	37.3	-52.7
3	PV	94.2	19.0	101.0	-	0	21.0	-19.0
4	PQ	47.8	-3.9	-	-	-	-	-
5	PQ	7.6	1.6	-	-	-	-	-
6	PV	11.2	7.5	107.0	-	0	16.5	-13.5
7	PQ	0	0	-	-	-	-	-
8	PV	0	0	109.0	-	0	24.0	- 6.0
9	PQ	29.5	16.6	-	-	-	-	-
10	PQ	9.0	5.8	-	-	-	-	-
11	PQ	3.5	1.8	-	-	-	-	-
12	PQ	6.1	1.6	-	-	-	-	-
13	PQ	13.5	5.8	-	-	-	-	-
14	PQ	14.9	5.0	-	-	-	-	-

Values of R, X and B in per-unit on 100 MVA base.

TABLE 10

D.C. Link Data for 14 Busbar Test System

	Inverter	Rectifier
v_l	0.0700	0.1740
x_l	0.0705	0.0700
x_v	0.0800	0.0700
x_t	0.0010	0.0010
b_t	0.1000	0.1000
γ_o	10	-
α_o	-	0
n	1.0000	0.9900
x_c	0.1510	0.1405

D.C. Line resistance, R = 0.015

Direct Current setting, i_{do} = 0.644

Current margin setting, Δi_{do} = 0.

All values in per-unit on 100 MVA base.

TABLE 11

Convergence Summary for 14 Busbar System Test Runs 1-7

Run number	1	2	3	4	5	6	7
Number of S.O.R. iterations performed after 1st D.C. link calculation	2	5	5	10	10	10	A.C. LOAD FLOW STUDY
Number of S.O.R. iterations performed after each subsequent D.C. link calculation	1	1	2	1	2	5	
Largest voltage change after 20 iterations. (p.u. x 10^4)	0.89	0.95	0.82	1.30	1.11	1.20	1.09

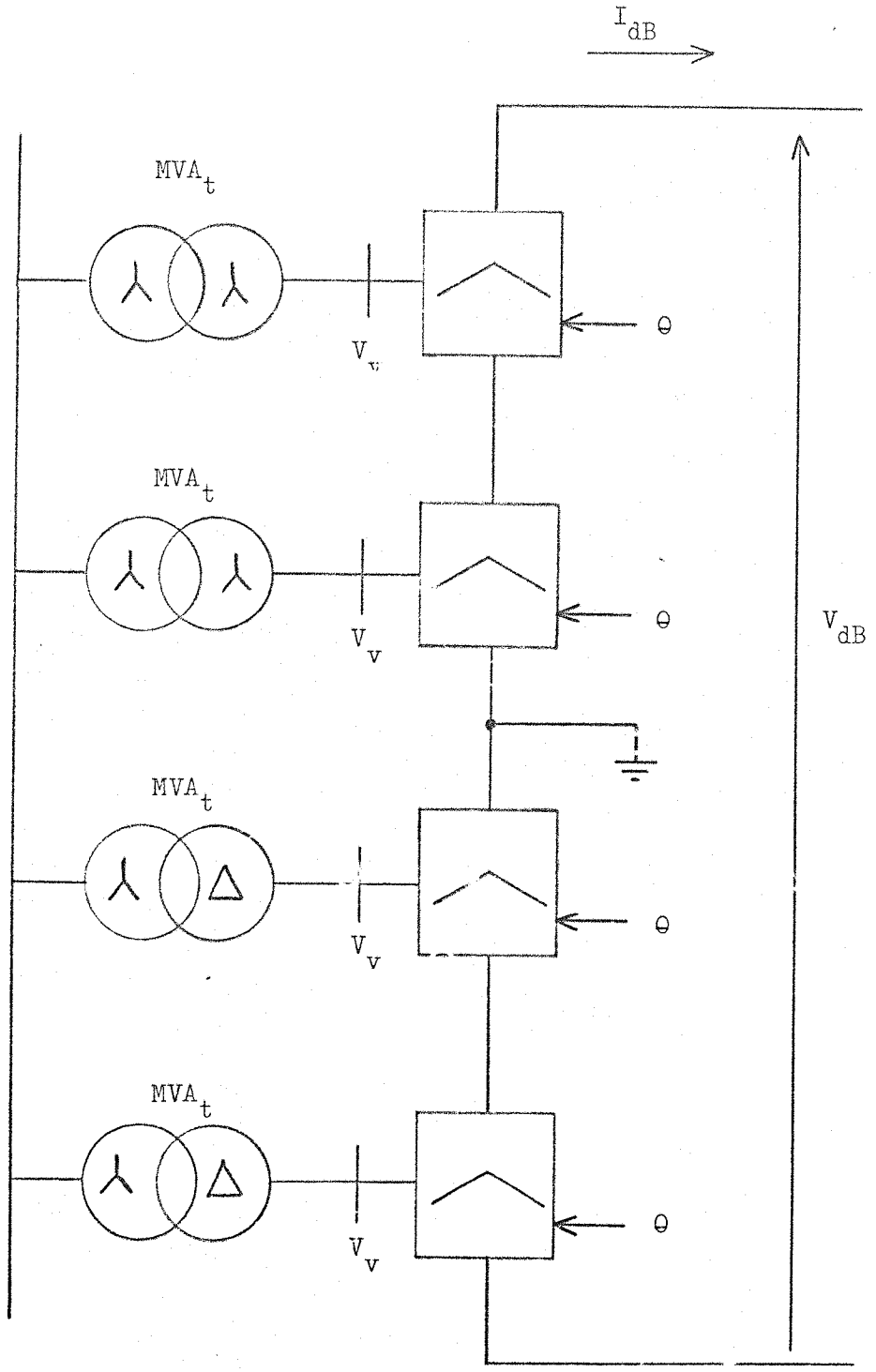

D.C. Voltage Base = V_{dB} = $(3\sqrt{2}/\pi)$

D.C. Power Base = P_{dB} = $MVA_t.N$

D.C. Current Base = I_{dB} = P_{dB}/V_{dB}

Fig. 1. Typical bi-polar 12-pulse converter station, with N = 4.

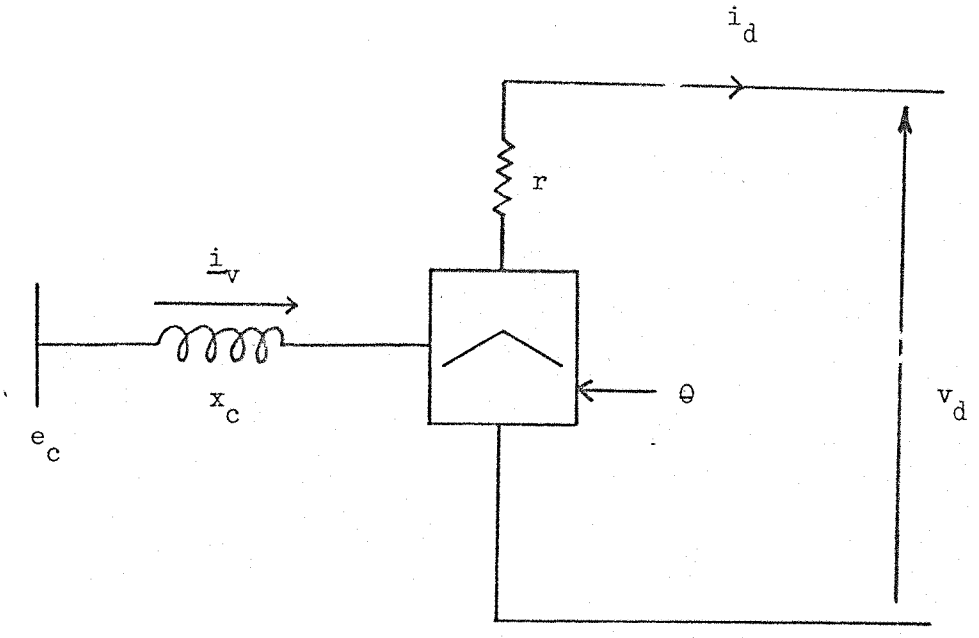

Fig. 2. Per-unit equivalent 6-pulse bridge.

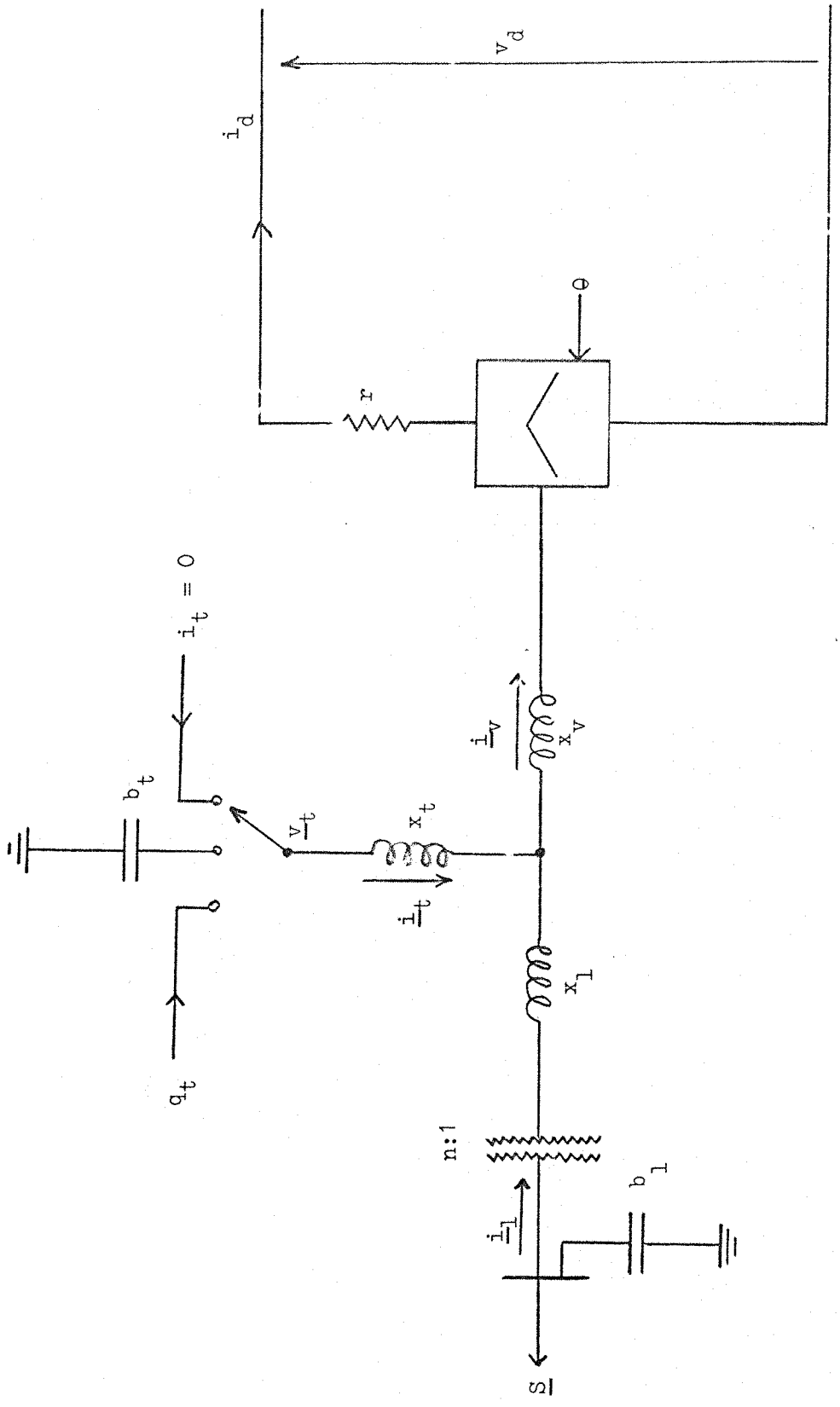

Fig. 3. Full Equivalent Circuit for converter station.
For 2 Winding Transformer $x_t = x_v = i_t = 0$.

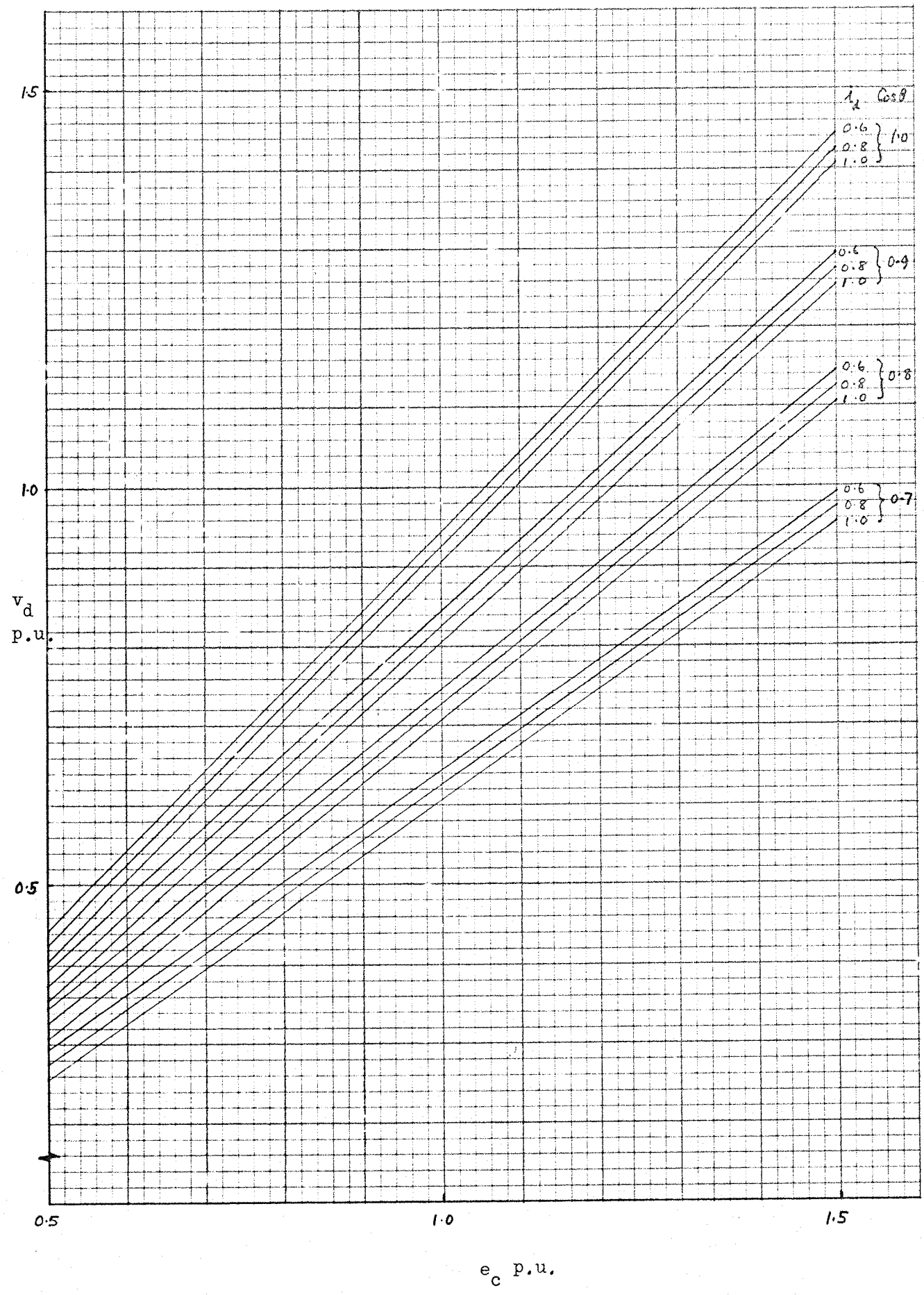

Fig. 4. Relationships between e_c, cos θ, i_d and v_d for DATA 1.

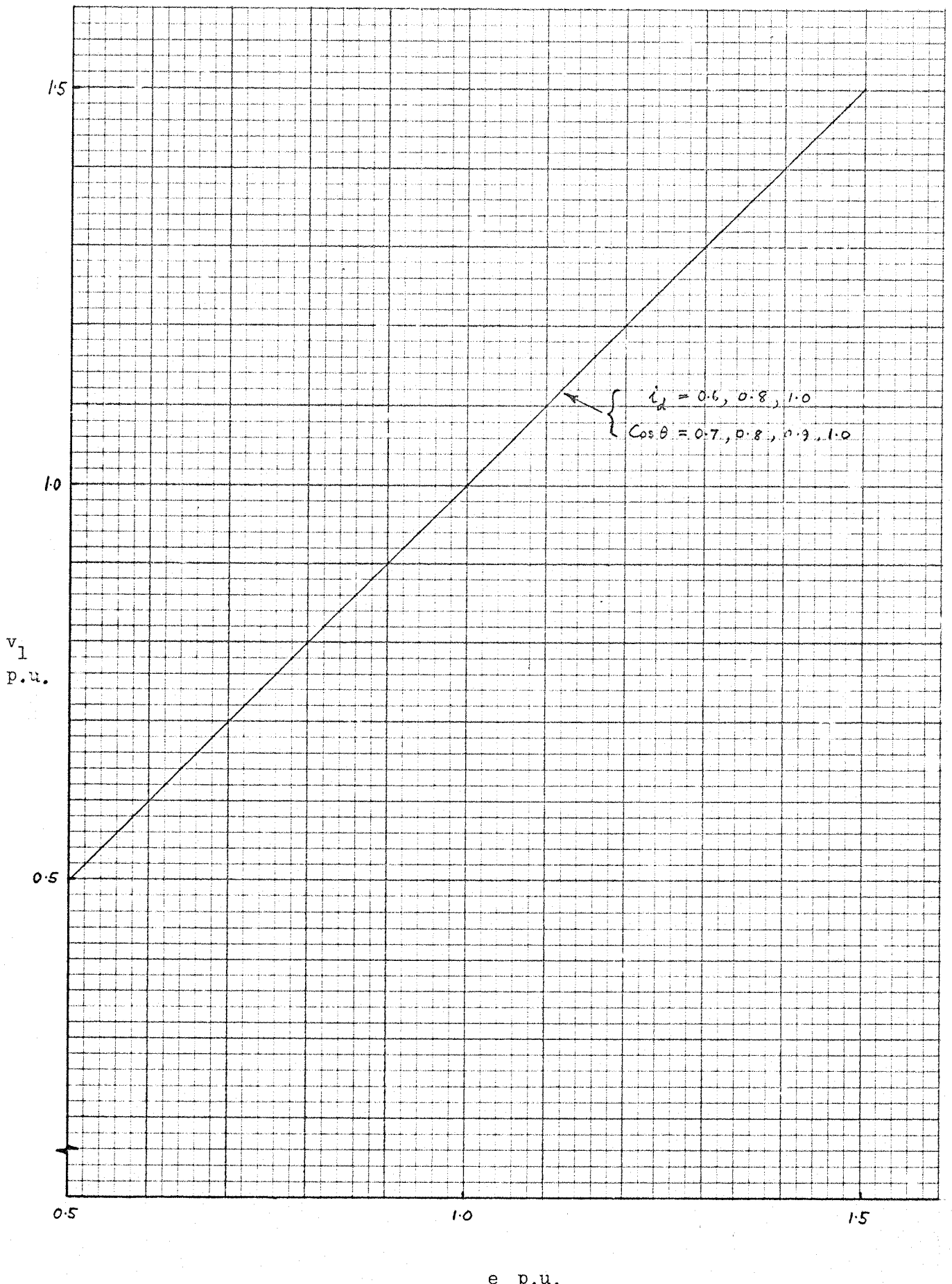

Fig. 5. Relationship between e_c, cos Θ, i_d and v_1 for DATA 1

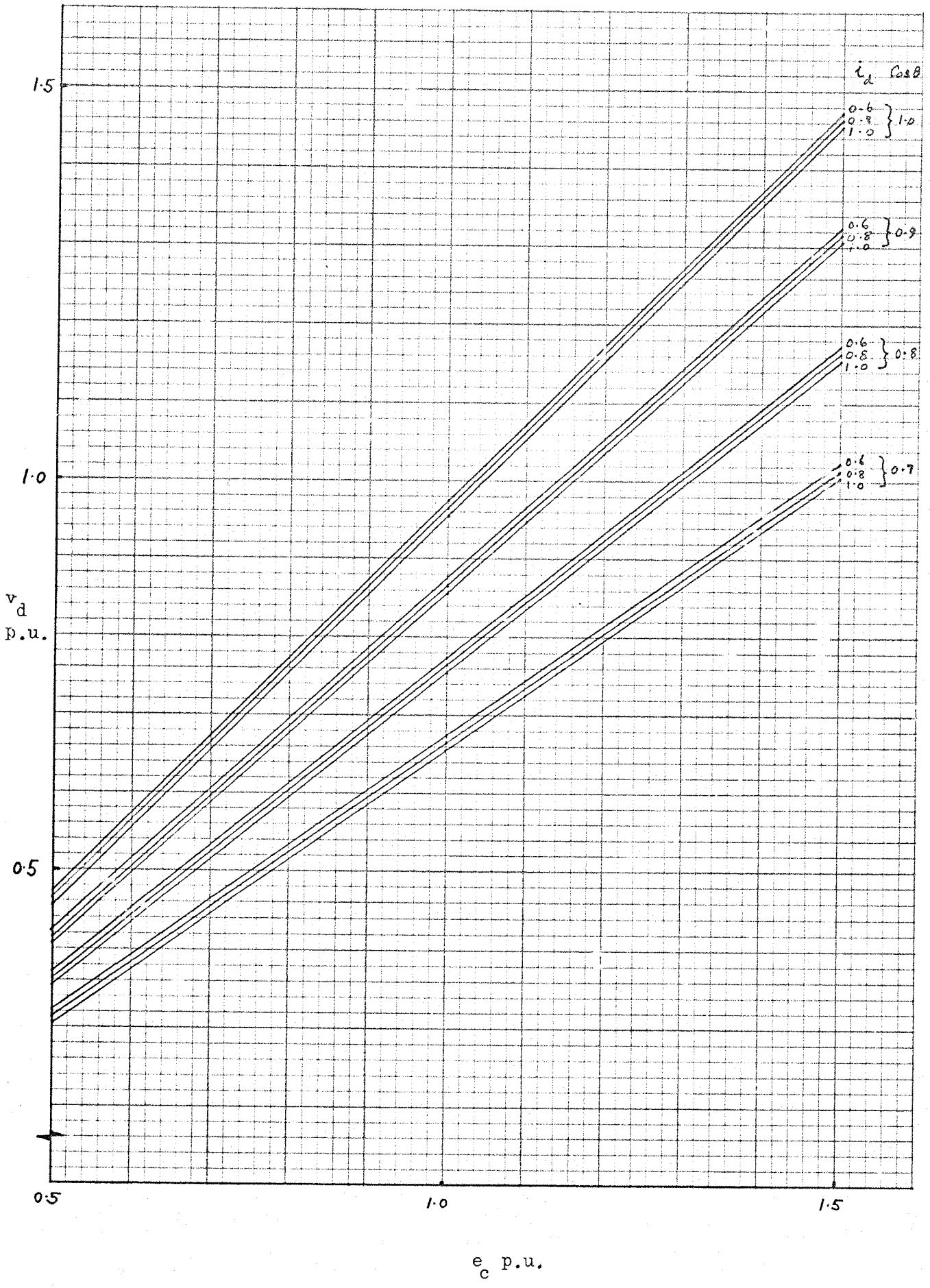

Fig. 6. Relationships between e_c, Cos Θ, i_d and v_d for DATA 2

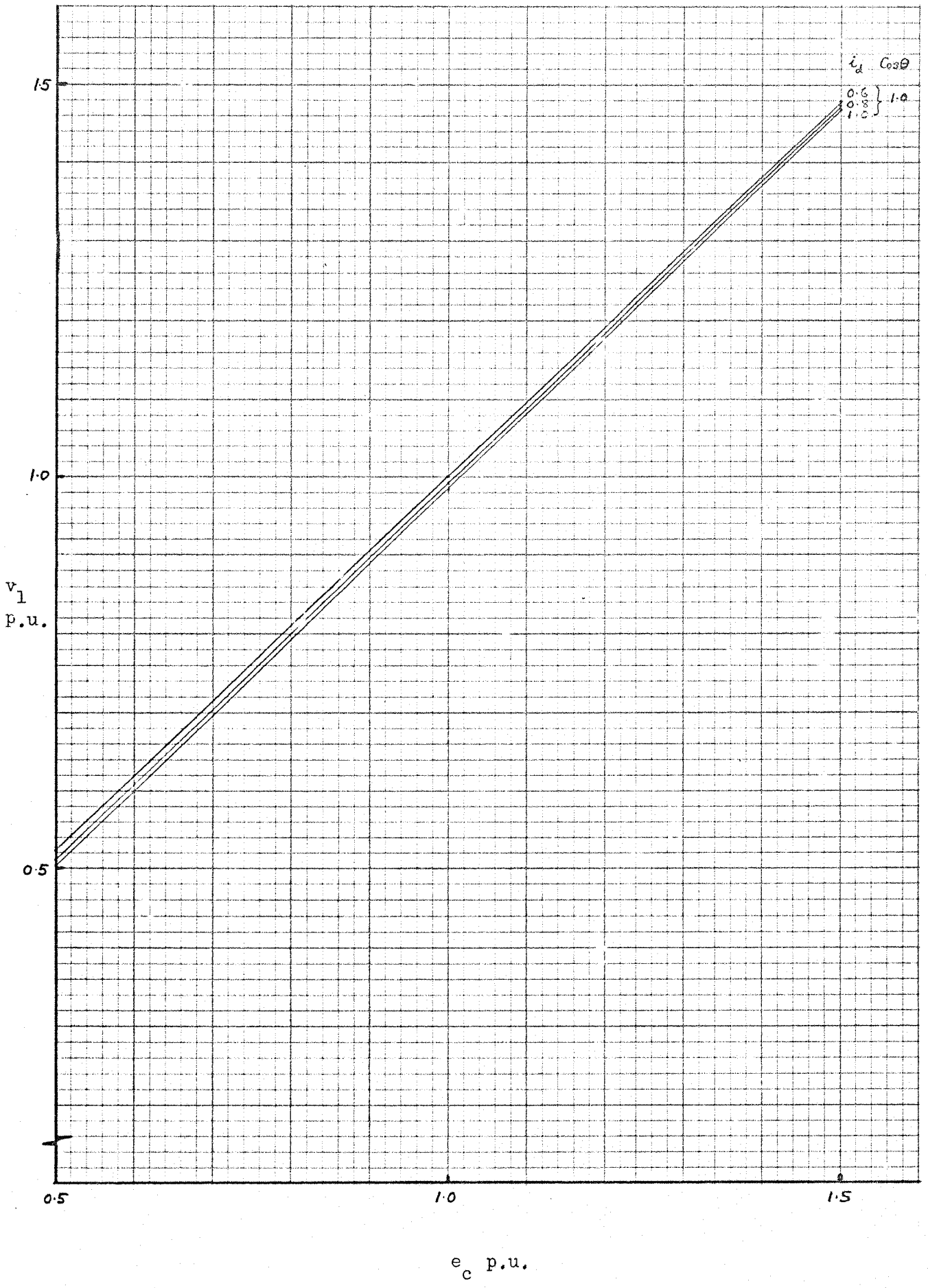

Fig. 7. Relationships between e_c, Cos θ, i_d and v_1 for DATA 2

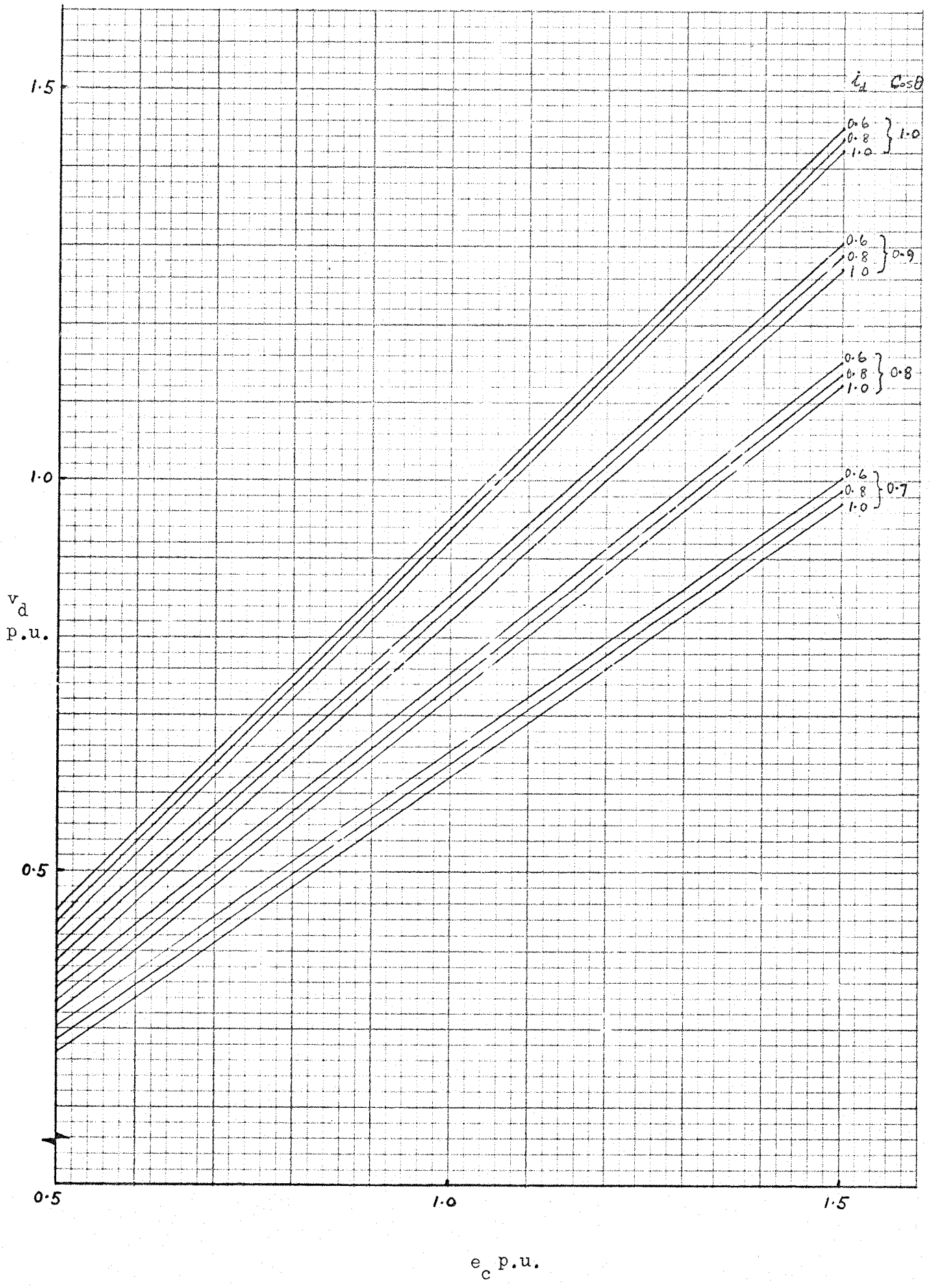

Fig. 8. Relationships between e_c, Cos θ, i_d and v_d for DATA 3

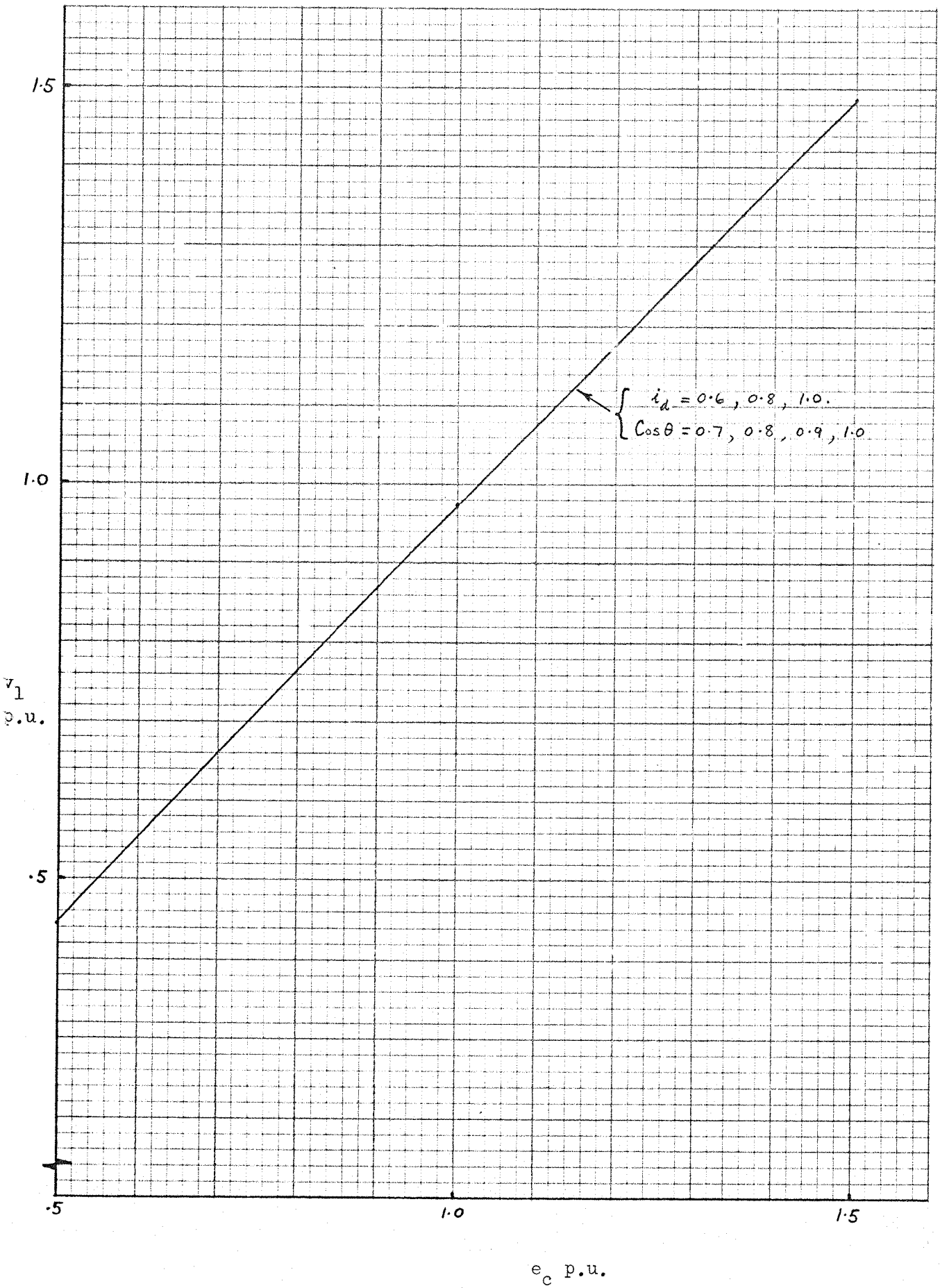

Fig. 9. Relationship between e_c, Cos θ, i_d and v_1 for DATA 3

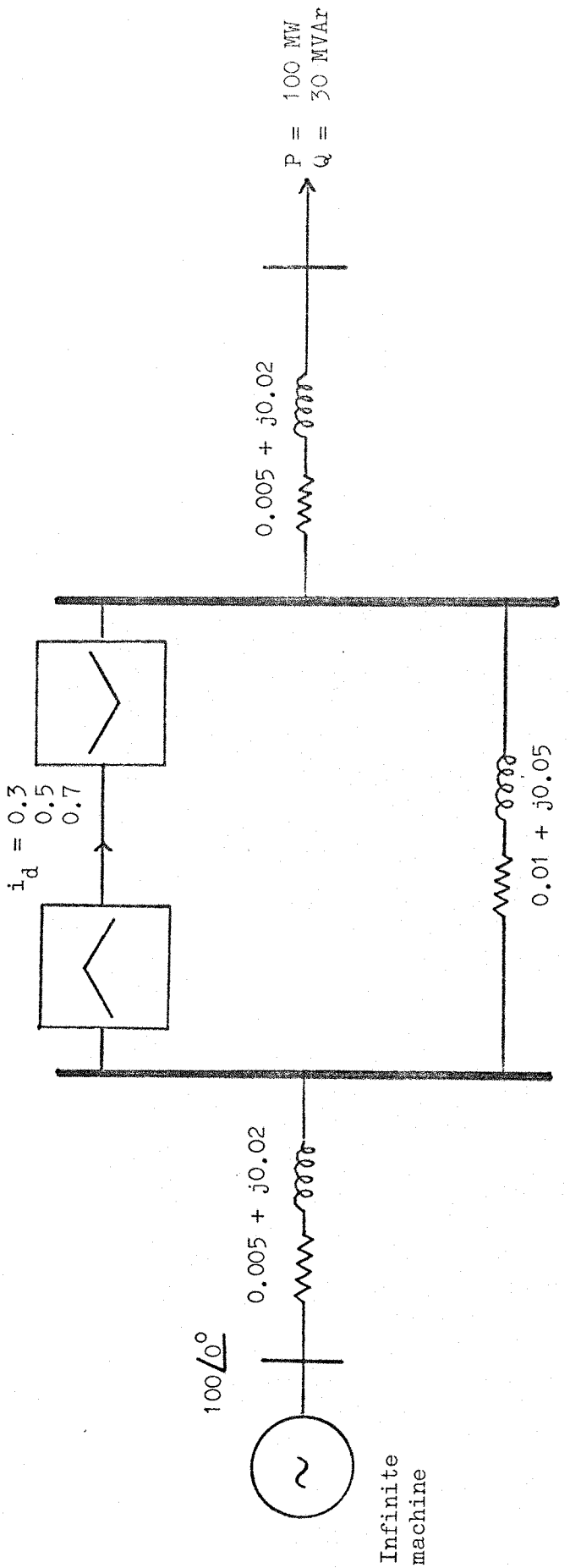

All impedance values in per-unit on 100 MVA.

Fig. 10. 4 Busbar A.C./D.C. Test System

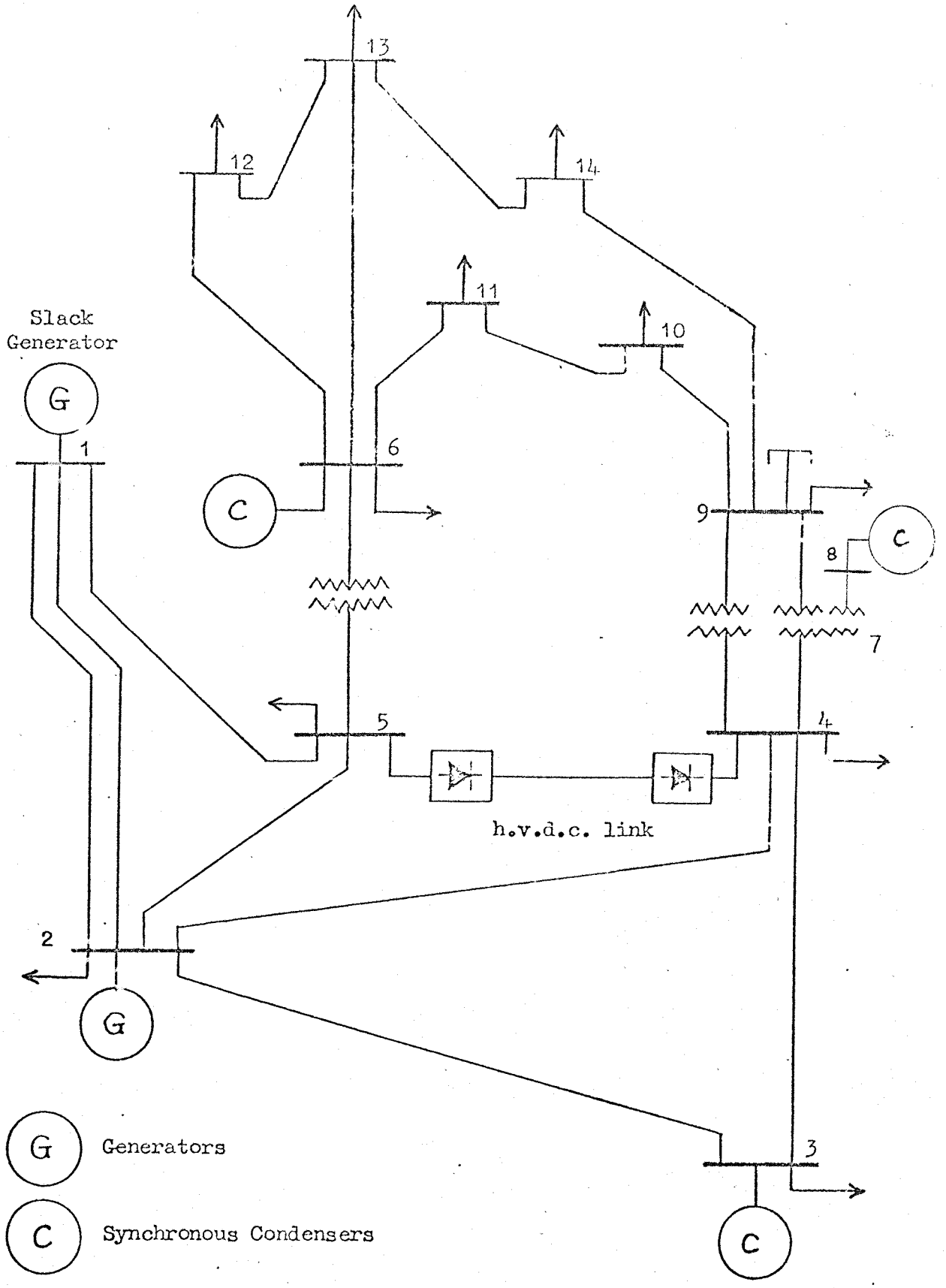

Fig. 11. 14 Busbar A.C./D.C. Test System

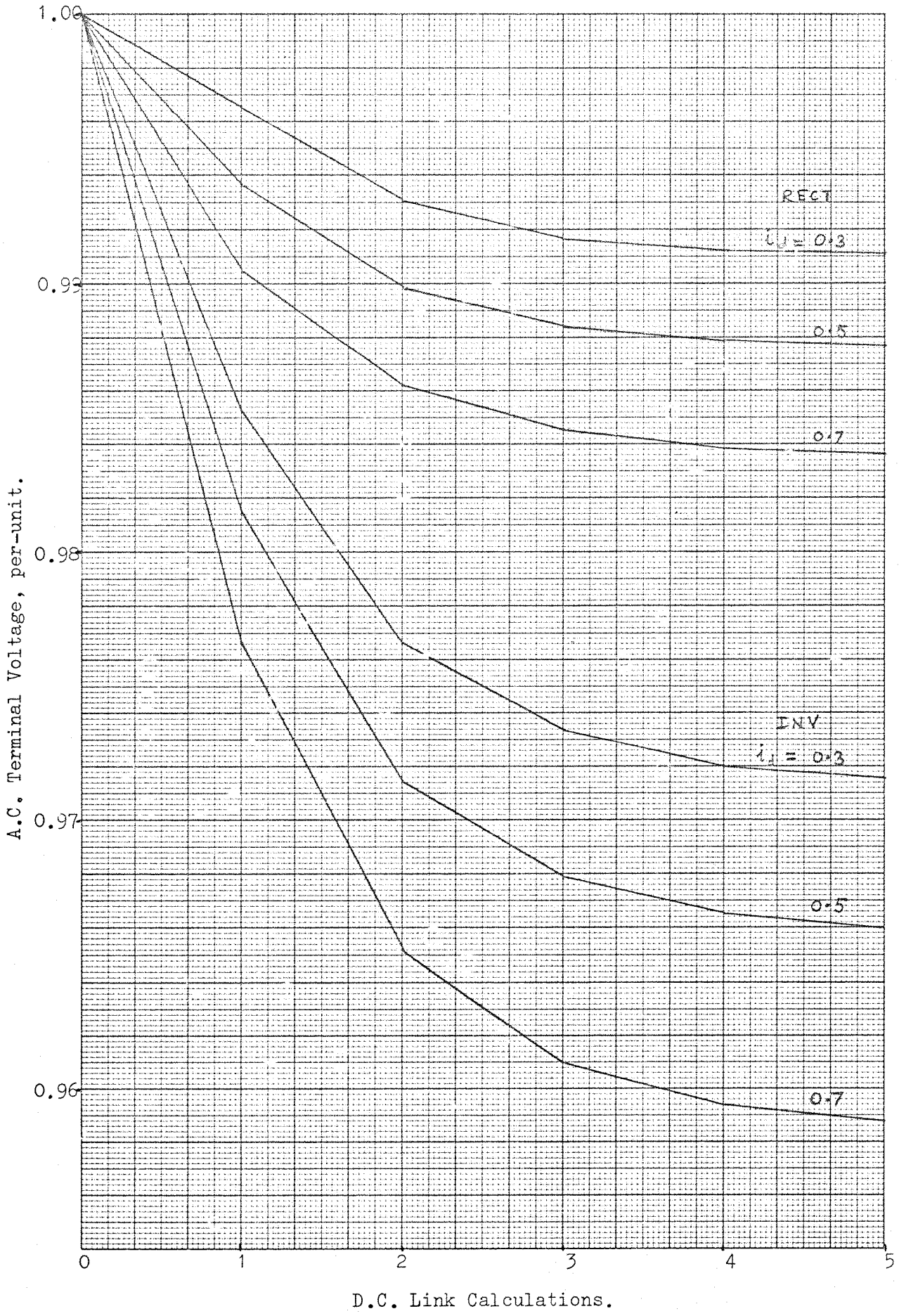

Fig. 12. Convergence of Converter A.C. Terminal Voltages for 4 Busbar A.C./D.C. Test System.

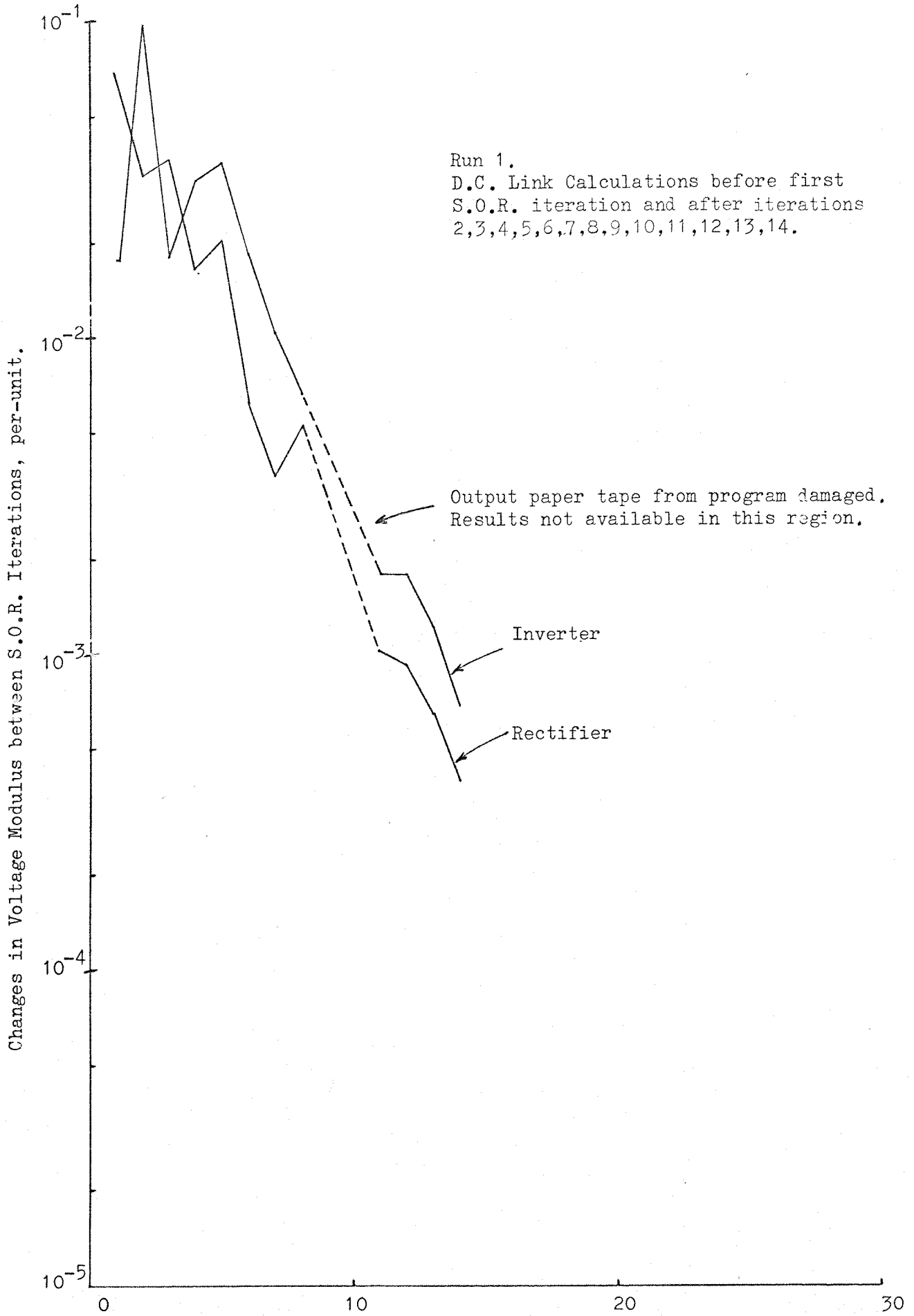

Fig. 13. Convergence of Converter A.C. Terminal Voltages for 14 Busbars A.C./D.C. Test System

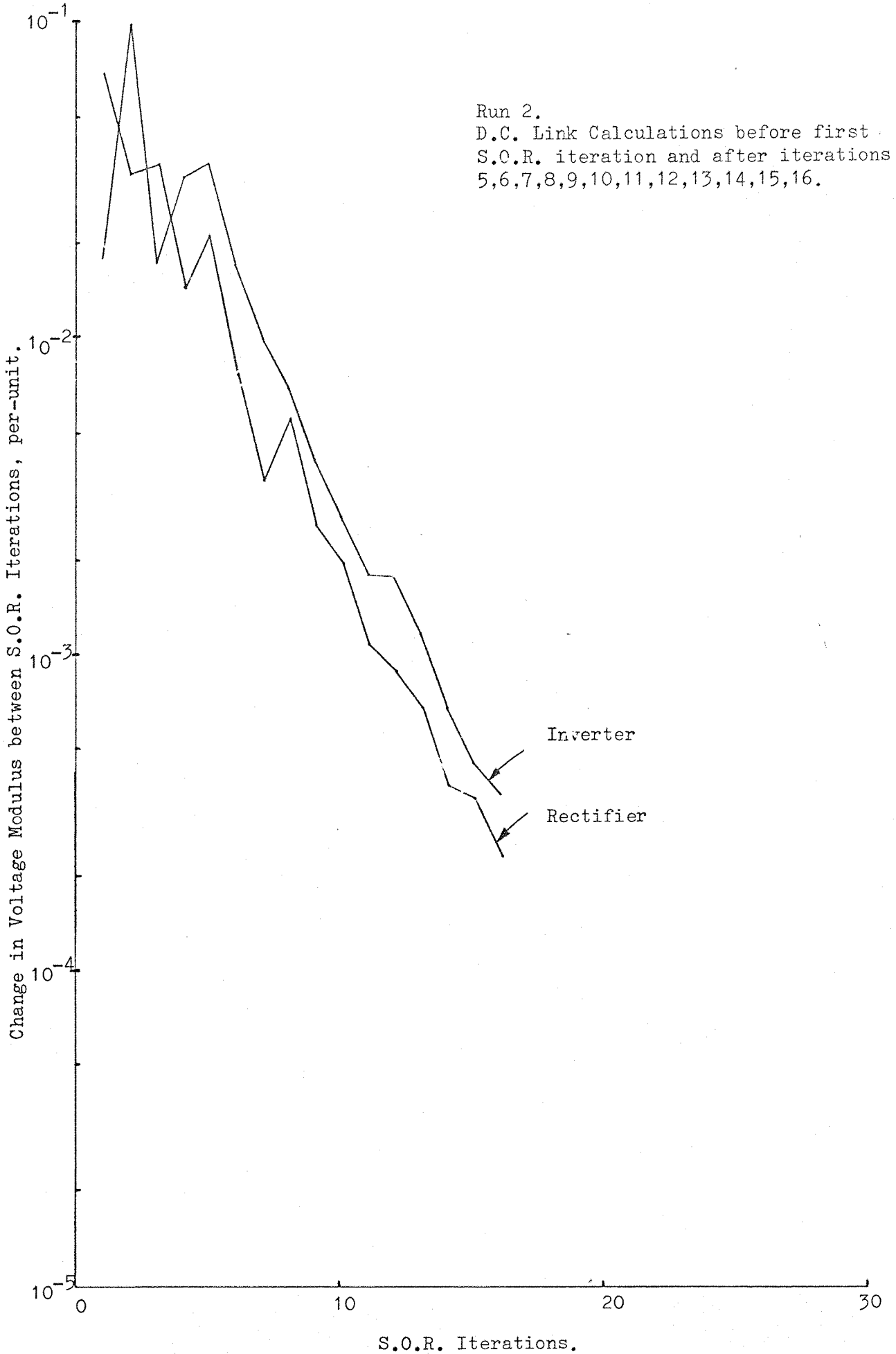

Fig. 14. Convergence of Converter A.C. Terminal Voltages for 14 Busbar A.C./D.C. Test System.

Fig. 15. Convergence of Converter A.C. Terminal Voltages for 14 Busbars A.C./D.C. Test System.

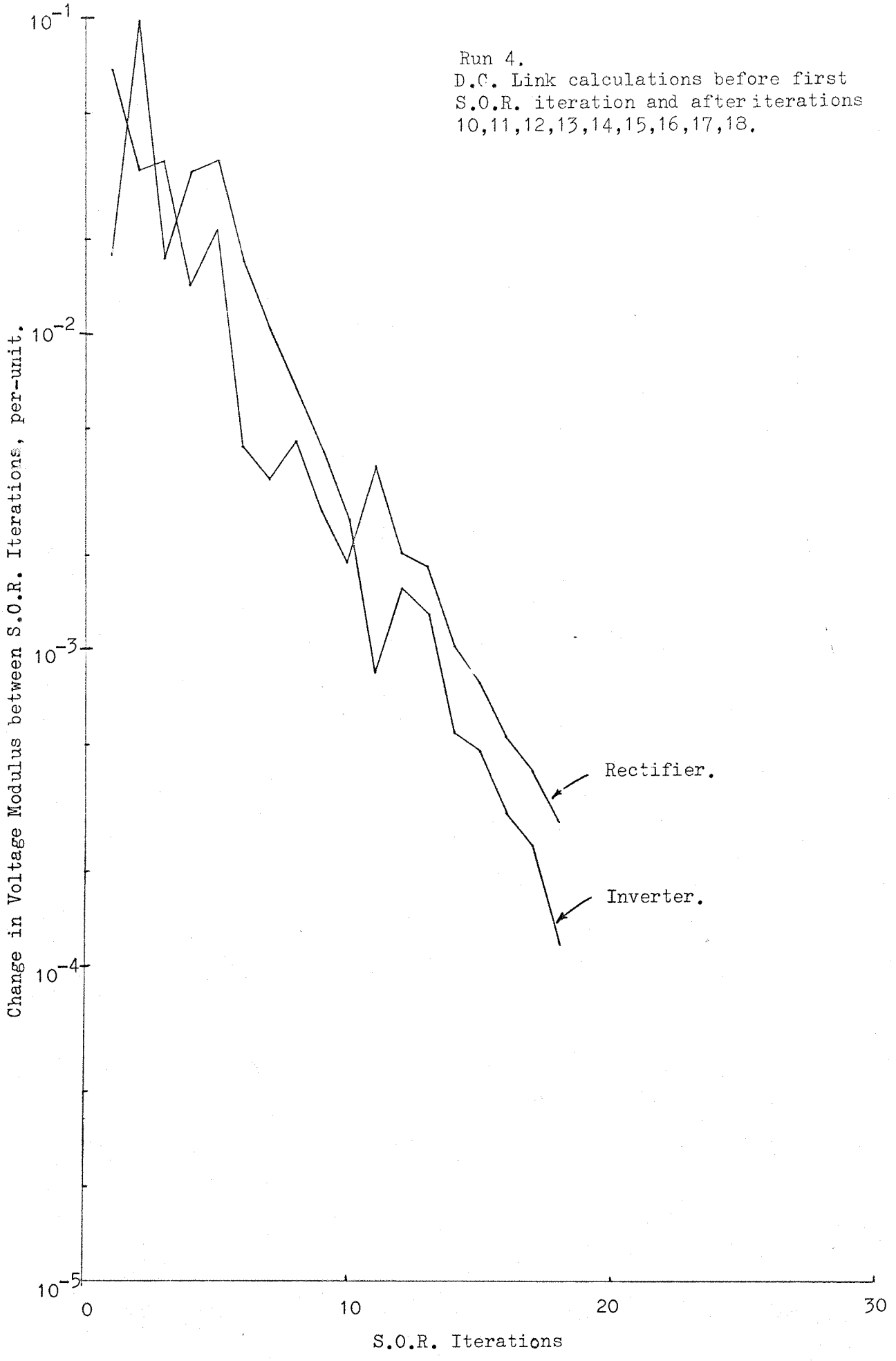

Fig. 16. Convergence of Converter A.C. Terminal Voltages for 14 Busbars A.C./D.C. Test system

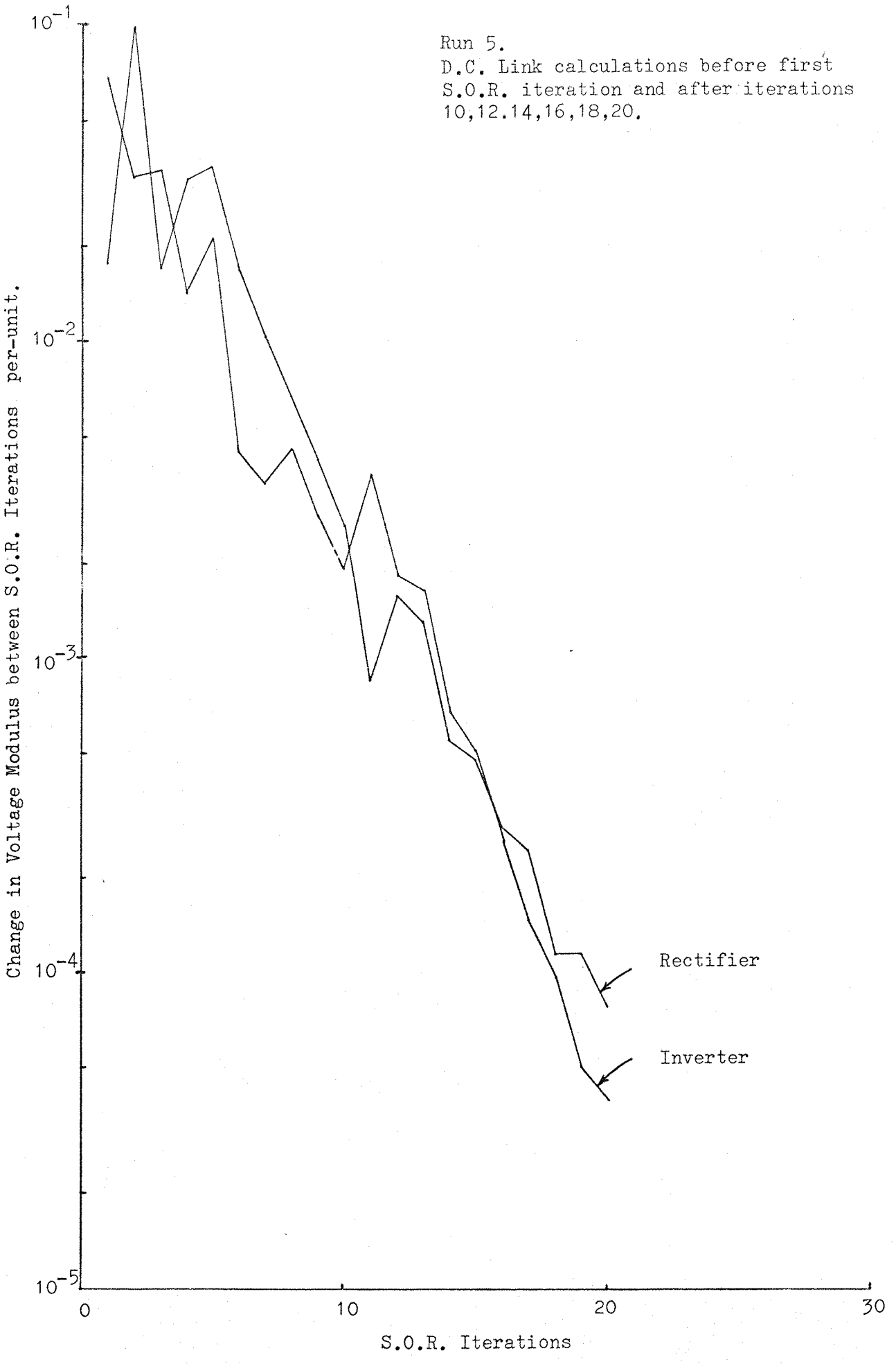

Fig. 17. Convergence of Converter A.C. Terminal Voltages for 14 Busbars A.C./D.C. Test System

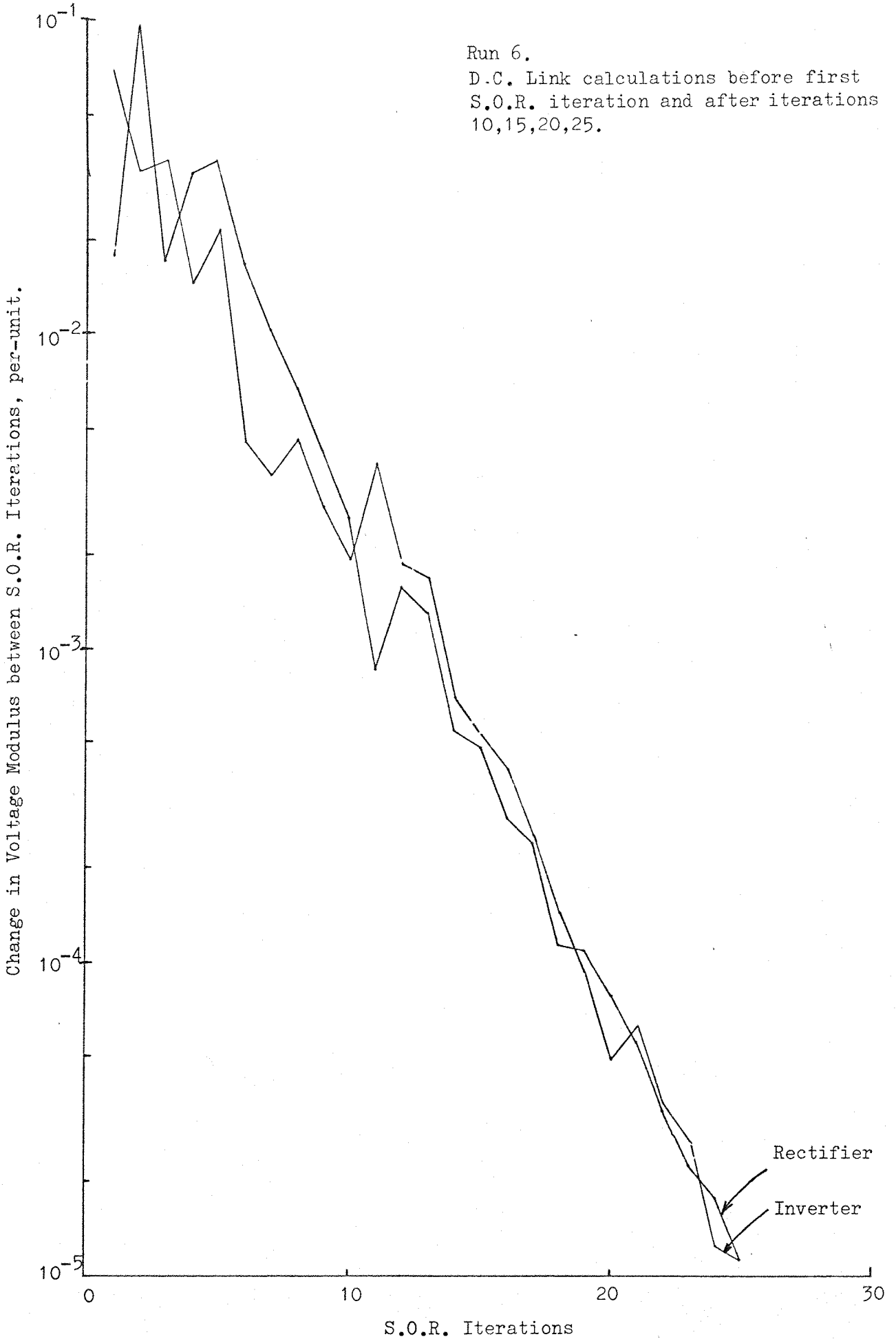

Fig. 18. Convergence of Converter A.C. Terminal Voltages for 14 Busbars A.C./D.C. Test System

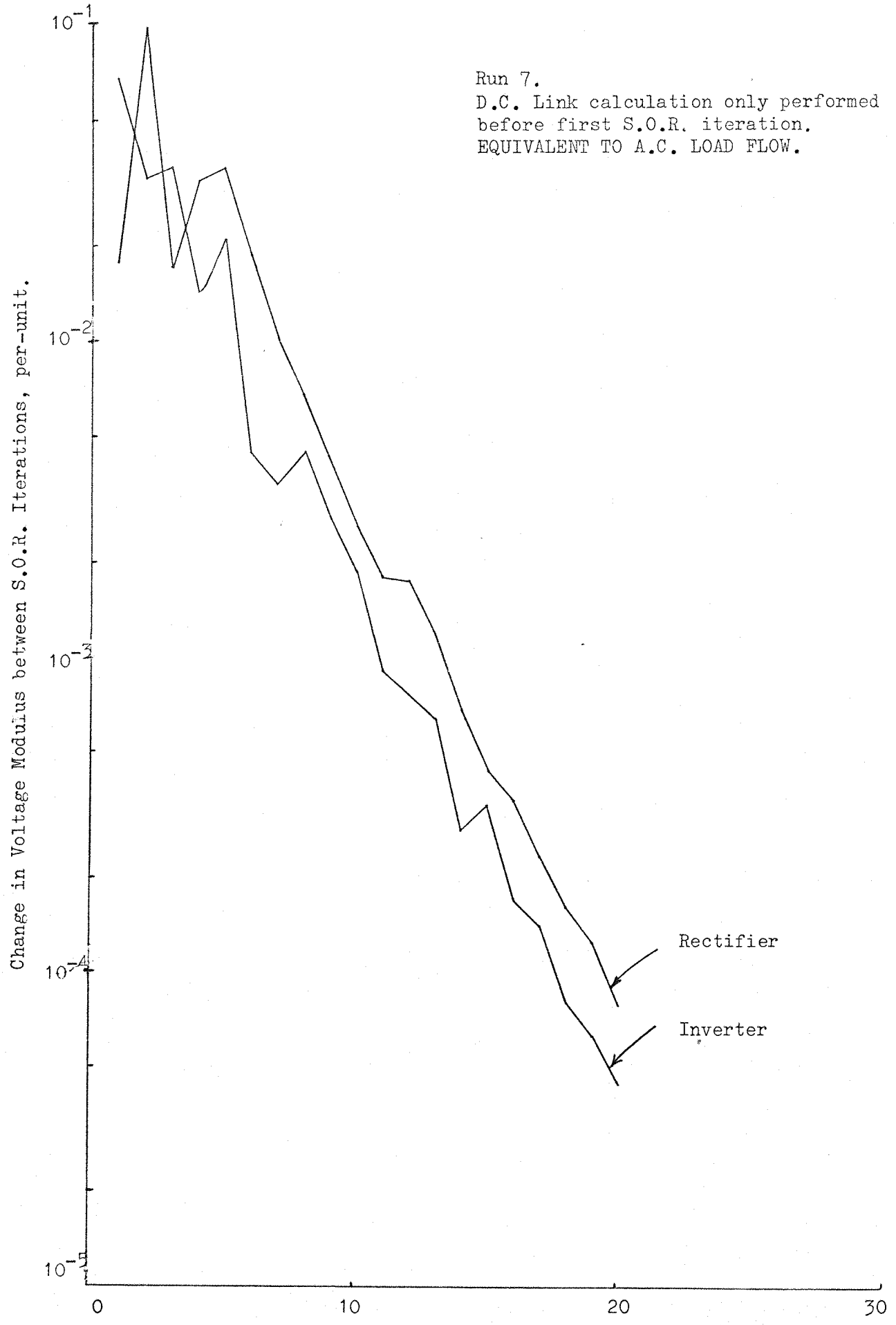

Fig. 19 Convergence of Converter A.C. Terminal Voltages for 14 Busbars A.C./D.C. Test System